Aus der Klinik für Augenheilkunde der Medizinischen Fakultät Charité – Universitätsmedizin Berlin

DISSERTATION

Epidermal growth factor (EGF) induces activation of transient receptor potential canonical (TRPC) channels in cultured human corneal epithelial cells (HCEC)

zur Erlangung des akademischen Grades
Doctor medicinae (Dr. med.)

vorgelegt der Medizinischen Fakultät
Charité – Universitätsmedizin Berlin

von

Julian Francisco Lopez

Datum der Promotion: 25.06.2023

Table of Contents

Abbreviations

5-FU	5-fluorouracil
ADP	adenosine diphosphate
ATPase	adenosine triphosphatase
BAEC	bovine aortic endothelial cells
BCEC	bovine corneal endothelial cells
BCTC	N-(4-tertiarybutylphenyl)-4-(3-chloropyridin-2-yl)tetrahydropyrazine-1(2H)-carboxamide
CAP	capsaicin
CCE	capacitative Ca^{2+} entry
DES	dry eye syndrome
DMEM	Dulbecco's Modified Eagle Medium
EBMD	epithelial basement membrane dystrophy
EGF	epidermal growth factor
EGFR	EGF receptor
EGTA	ethylene glycol-bis(β-aminoethyl ether)-N,N,N′,N′-tetraacetic acid
ER	endosplasmic reticulum
FCS	fetal calf serum
Fura-2AM	Fura-2-acetoxymethyl ester
GPCR	G protein-coupled receptor
HCEC	human corneal epithelial cells
HCK	human corneal keratocytes
HEK-293	human embryonic kidney 293 cells
HEPES	4-(2-hydroxyethyl)-1-piperazineethanesulfonic acid
HP	holding potential
IFN-α2b	interferon alpha 2b
IP_3/$InsP_3$	inositol 1,4,5-trisphosphate

$IP_3R/InsP_3R$	IP_3 receptor
LSC	limbal stem cells
MMC	mitomycin C
NSCLC	non-small cell lung carcinoma
ORAI1	Ca^{2+} release-activated Ca^{2+} channel protein 1
OSSN	ocular surface squamous neoplasia
PASMC	pulmonary artery smooth muscle cells
PBS	phosphate buffered saline
PLCβ	phospholipase C beta
PLCγ	phospholipase C gamma
PMCA	plasma membrane Ca^{2+}-ATPase
RCEC	rabbit corneal epithelial cells
RCF	relative centrifugal force
ROI	region of interest
Rs	series resistance
RTK	receptor tyrosine kinase
RyR	ryanodine receptor
SEM	standard error of mean
SERCA	sarco/endoplasmic reticulum Ca^{2+}-ATPase
SKF 96365	1-[β-(3-(4-Methoxyphenyl)propoxy)-4-methoxyphenethyl]-1H-imidazole hydrochloride
SOC	store-operated channel
STIM1	stromal interaction molecule 1
SV-40	simian virus 40
TRP	transient receptor potential
TRPA	TRP ankyrin
TRPC	TRP canonical

TRPM	TRP melastatin
TRPML	TRP mucolipin
TRPN	TRP NOMP, no mechanopotential TRP
TRPP	TRP polycystic
TRPs	transient receptor potential channels
TRPV	TRP vanilloid
UV	ultraviolet
VDCC	voltage-dependent Ca^{2+} channel
VEGF	vascular endothelial growth factor
XLHED	X-linked hypohidrotic ectodermal dysplasia
ZO-1	zonula occludens-1

List of figures

Abstract

Human corneal epithelial cells (HCEC), which are found on the outermost layer of the human cornea, play a vital role in maintaining vision. Research over the years has shown that various transient receptor potential channels (TRPs) are expressed on the surface of many ocular cells including the HCEC. With their intracellular and extracellular domains, TRPs are capable of converting external stimuli into signal transduction pathways within the cell. These channels play a significant role in Ca^{2+} regulation and mediate numerous intracellular processes by controlling the flow of Ca^{2+} ions across the cell membrane. Interestingly, studies have shown that growth factors can influence Ca^{2+} regulation via interaction with certain TRPs. As epidermal growth factor (EGF) in particular has been shown to promote healing of damaged corneal epithelial tissue, a closer study of the effect of EGF on HCEC would be useful. This study aims to investigate the influence EGF on Ca^{2+} regulation in cultured HCEC and the involvement of TRPs in this process. Fluorescence Ca^{2+} imaging of SV-40 transfected HCEC yielded the following results: Application of 50 ng/ml EGF caused a significant increase in intracellular Ca^{2+} concentration. This increase was significantly suppressed in the presence of the TRP canonical (TRPC) channel antagonist SKF 96365 (10–20 µM). When a Ca^{2+}-free measuring solution was used, no increase in intracellular Ca^{2+} concentration was observed upon application of 50 ng/ml EGF. Patch-clamp measurement of whole-cell currents revealed an increase in inward and outward currents through the cell membrane upon application of 50 ng/ml EGF. This EGF-induced increase in currents was suppressed in the presence of 20 µM SKF 96365. Taken together, this study demonstrates the involvement of TRPC channels in EGF-induced Ca^{2+} increase in HCEC. The results also suggest that this effect is due to EGFR-associated activation of TRPC channels on the cell membrane rather than the depletion of intracellular Ca^{2+} stores.

Zusammenfassung

Humane Hornhautepithelzellen (HCEC), die sich auf der äußersten Schicht der menschlichen Hornhaut befinden, spielen eine wichtige Rolle bei der Aufrechterhaltung des normalen Sehvermögens. Die Forschung im Laufe der Jahre zeigte, dass unterschiedliche Transient-Receptor-Potential-Kanäle (TRPs) in Zellen der Augenoberfläche einschließlich der HCEC exprimiert sind. Mit ihrer intra- und extrazellulären Domäne können TRPs externe Stimuli in Signaltransduktionswege innerhalb der Zelle umwandeln. Diese Kanäle spielen eine wichtige Rolle bei Ca^{2+}-Regulation und vermitteln zahlreiche intrazelluläre Prozesse, indem sie den Fluss von Ca^{2+}-Ionen durch die Zellmembran steuern. Interessanterweise zeigten Studien, dass Wachstumsfaktoren die Ca^{2+}-Regulation durch Wechselwirkung mit bestimmten TRPs beeinflussen können. Da insbesondere der epidermale Wachstumsfaktor (EGF) gezeigt hat, dass er die Heilung von geschädigtem Hornhautepithelgewebe fördert, wäre eine nähere Untersuchung der Wirkung von EGF auf HCEC nützlich. Ziel dieser Studie ist es, den Einfluss von EGF auf die Ca^{2+}-Regulation in kultivierten HCEC und die Beteiligung von TRPs an diesem Prozess zu untersuchen. Die Fluoreszenz-Ca^{2+}-Image-Messungen von SV-40-transfizierten HCEC ergaben folgende Ergebnisse: Die extrazelluläre Applikation von 50 ng/ml EGF führte zu einem signifikanten Anstieg der intrazellulären Ca^{2+}-Konzentration. Dieser Anstieg wurde in Gegenwart des kanonischen TRP (TRPC)-Kanalantagonisten SKF 96365 (10–20 µM) deutlich unterdrückt. Bei Verwendung einer Ca^{2+}-freien Messlösung löste 50 ng/ml EGF keinen Anstieg der intrazellulären Ca^{2+}-Konzentration aus. Patch-Clamp Messungen von Ganzzellströmen ergaben einen Anstieg der Ein- und Ausströme durch die Zellmembran nach Zugabe von 50 ng/ml EGF. Dieser EGF-induzierte Anstieg der Ströme wurde in Gegenwart von 20 µM SKF 96365 unterdrückt. Insgesamt deutet diese Studie eine Beteiligung von TRPC Kanäle am EGF-induzierten Ca^{2+}-Anstieg in HCEC an. Die Ergebnisse weisen auch darauf hin, dass dieser Effekt eher auf ein EGFR-assoziierte Aktivierung von TRPC Kanäle auf der Zellmembran zurückzuführen ist, als auf die Entleerung von intrazellulären Ca^{2+}-Speichern.

1 Introduction

1.1 The corneal epithelium

The cornea serves as a transparent structural barrier on the outer surface of the eye, which protects it from infections as well as refracts light entering the eye. The human cornea can be subdivided into 5 layers; the endothelium, Descemet membrane, stroma, Bowman membrane and epithelium (1) (see Fig. 1).

The corneal epithelium is a non-keratinised, stratified squamous epithelium. The glycocalyx of these cells interact with the mucin layer of tears, enabling the tear film to spread evenly across the eye during blinking (2). Damage to this layer can cause pain, inflammation or loss of vision (3). The corneal epithelium also regulates the movement of electrolytes and water from the stroma to the tear film. This function, together with transendothelial fluid transport, prevents excessive fluid build-up in the stroma, maintaining corneal transparency (4-6).

Corneal epithelial cell dysfunction is a common pathophysiological component of a number of corneal diseases. In dry eye syndrome (DES), inflammatory responses on the ocular surface can lead to apoptosis of corneal epithelial cells and thinning of the epithelial layer (7-9). Similarly, pro-inflammatory cytokines released by corneal epithelial cells in response to herpetic infections can cause scarring and damage the cornea, resulting in loss of vision (10). Corneal epithelial cells are also implicated in various genetic disorders. In mice with X-linked hypohidrotic ectodermal dysplasia (XLHED), expression of tight junction proteins zonula occludens-1 (ZO-1) and claudin-1 was found to be reduced in corneal epithelial cells, causing a loss of epithelial integrity and dysfunction of the epithelial barrier (11). The effects of a dysfunctional corneal epithelial layer are particularly evident in patients with limbal stem cell deficiency (LSCD). Limbal stem cells (LSC) are stem cells found in the limbus, the border between the cornea and the conjunctiva. These cells are responsible for the regeneration of the corneal epithelium. In LSCD, the lack of functional LSC prevents the epithelium from healing effectively. As a result, persistent epithelial defects may occur, as well as neovascularisation, inflammation and scarring of the cornea. It can also result in corneal

conjunctivalisation, a process in which corneal epithelial cells are gradually replaced with conjunctival epithelial cells, reducing corneal transparency and impairing vision (12-14).

As the outermost layer of the cornea, the corneal epithelium is exposed to the environment and is particularly vulnerable to injuries. Defects to this layer are relatively common. In fact, corneal epithelial defects and abrasions are among the most frequently encountered ocular pathologies (15). Furthermore, treatment of many ocular pathologies involve application of drugs directly to the surface of the eye, and the corneal epithelium is the first layer that comes into contact with these substances. One such drug is cyclosporine A, which is applied topically to reduce inflammation in a host of ocular diseases including atopic and vernal keratoconjunctivitis, ulcerative keratitis, ligneous conjunctivitis, DES and Mooren's ulcer (16, 17). Ocular surface squamous neoplasia (OSSN) is a group of corneal, conjunctival and limbal epithelial malignancies, which can also be treated topically. Chemotherapeutic agents such as mitomycin C (MMC) and 5-fluorouracil (5-FU), as well as immunotherapeutic agents like interferon alpha 2b (IFN-α2b) are often applied directly to the ocular surface as part of primary treatment for OSSN (18, 19).

In summary, the corneal epithelium is an essential component of the eye due to its role in maintaining ocular function, its involvement in the pathophysiology of many ocular diseases and its anatomical significance as an external layer. Studying the characteristics of this layer at the cellular level would greatly enhance our understanding corneal pathologies and enable the development of effective treatment strategies in the future.

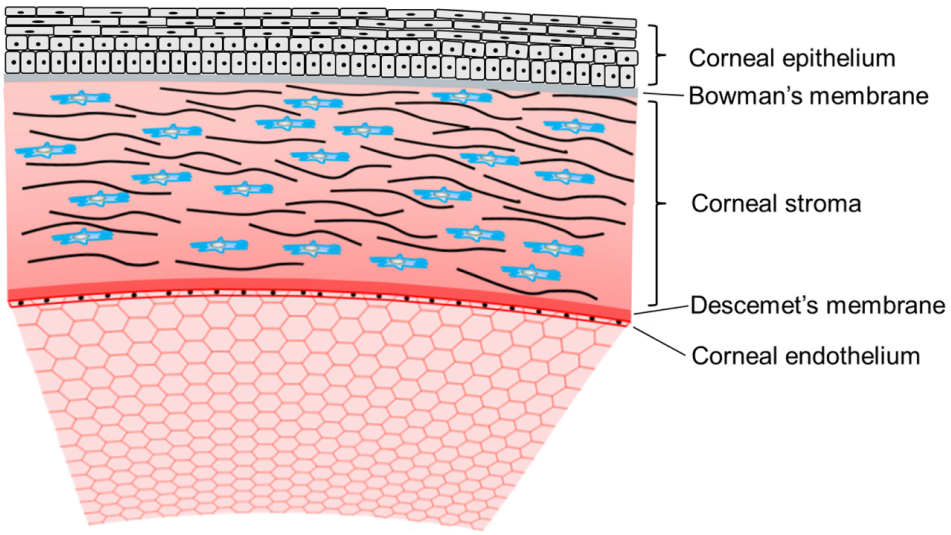

Fig. 1: The 5 layers of the human cornea. (Illustration by Chen et al., 2018 (20), reused with the kind permission of © IOP Publishing Ltd.)

1.2 Intracellular Ca^{2+} regulation

Ca^{2+} is one of the most important signal particles within the cell and many intracellular physiological processes are Ca^{2+}-dependent. Among other functions, Ca^{2+} is significantly involved in gene expression, signal transduction and metabolic pathways (21). Its importance is also evident in cell culture. In a study of immortalised human corneal epithelial cells (HCEC) *in vitro*, varying the levels of glucose and Ca^{2+} in the culture medium affected the rate of cell proliferation and differentiation, expression of focal adhesions, as well as the metabolism of the cells (22).

Various cellular protein structures facilitate the movement of Ca^{2+} in the cell. One way Ca^{2+} enters the cytosol is through Ca^{2+} channels located on the cell membrane. Physical or chemical stimuli can increase the open probability of these channels, allowing more Ca^{2+} to diffuse along a concentration gradient from the extracellular into the intracellular space (23) (see Fig. 2). Transient receptor potential channels (TRPs), for example, are a diverse group of ion channels which play an important role in Ca^{2+} regulation. These channels will be discussed further in Chapter 1.3.

Ca^{2+} may also enter the cytosol from intracellular Ca^{2+} stores in the endoplasmic reticulum (ER) of the cell. When exposed to their respective ligands like hormones, growth factors or neurotransmitters, receptors on the cell membrane such as G protein-

coupled receptors (GPCRs) and receptor tyrosine kinases (RTKs) are activated. The GPCRs then activate phospholipase C beta (PLCβ), while the RTKs activate phospholipase C gamma (PLCγ). These phospholipases generate second messengers such as inositol 1,4,5-trisphosphate (IP_3), which binds to and activates the IP_3 receptor (IP_3R). This receptor is a membrane glycoprotein complex, which behaves as an intracellular Ca^{2+}-release channel on the membrane of the ER. The activated channel then opens, allowing Ca^{2+} to flow from the stores into the cytosol (24) (see Fig. 2).

The ryanodine receptor (RyR) is another type of intracellular Ca^{2+}-release channel localised on the membrane of the ER, which is involved in Ca^{2+} regulation. When cytosolic Ca^{2+} increases, RyRs detect the change and open to allow an efflux of Ca^{2+} from the stores in a positive feedback mechanism called Ca^{2+}-induced Ca^{2+} release. A further increase in Ca^{2+} may cause the RyRs to close, halting the efflux of Ca^{2+} from the stores. RyRs are also responsible for store overload-induced Ca^{2+} release, a mechanism where RyRs detect the filling state of Ca^{2+} stores and open in response to high store Ca^{2+} levels, allowing the excess Ca^{2+} to flow into the cytosol (25, 26) (see Fig. 2).

When excess Ca^{2+} is no longer needed in the cytosol, is sequestered back into the stores via sarco/endoplasmic reticulum Ca^{2+}-ATPases (SERCA) on the ER and removed from the cell via plasma membrane Ca^{2+}-ATPases (PMCA) and Na^{+}/Ca^{2+} exchangers on the cell membrane (24) (see Fig. 2).

The concentration and distribution of Ca^{2+}, as well as the speed and duration of Ca^{2+} flux allow different signaling pathways to be uniquely controlled in the cell (24). To maintain optimal function and carry out their physiological processes, cells require an intricate system of Ca^{2+} regulation. Ca^{2+} channels are crucial components of this regulation; their activity directly affects the flux of Ca^{2+}, which in turn modulates numerous intracellular Ca^{2+}-dependent mechanisms.

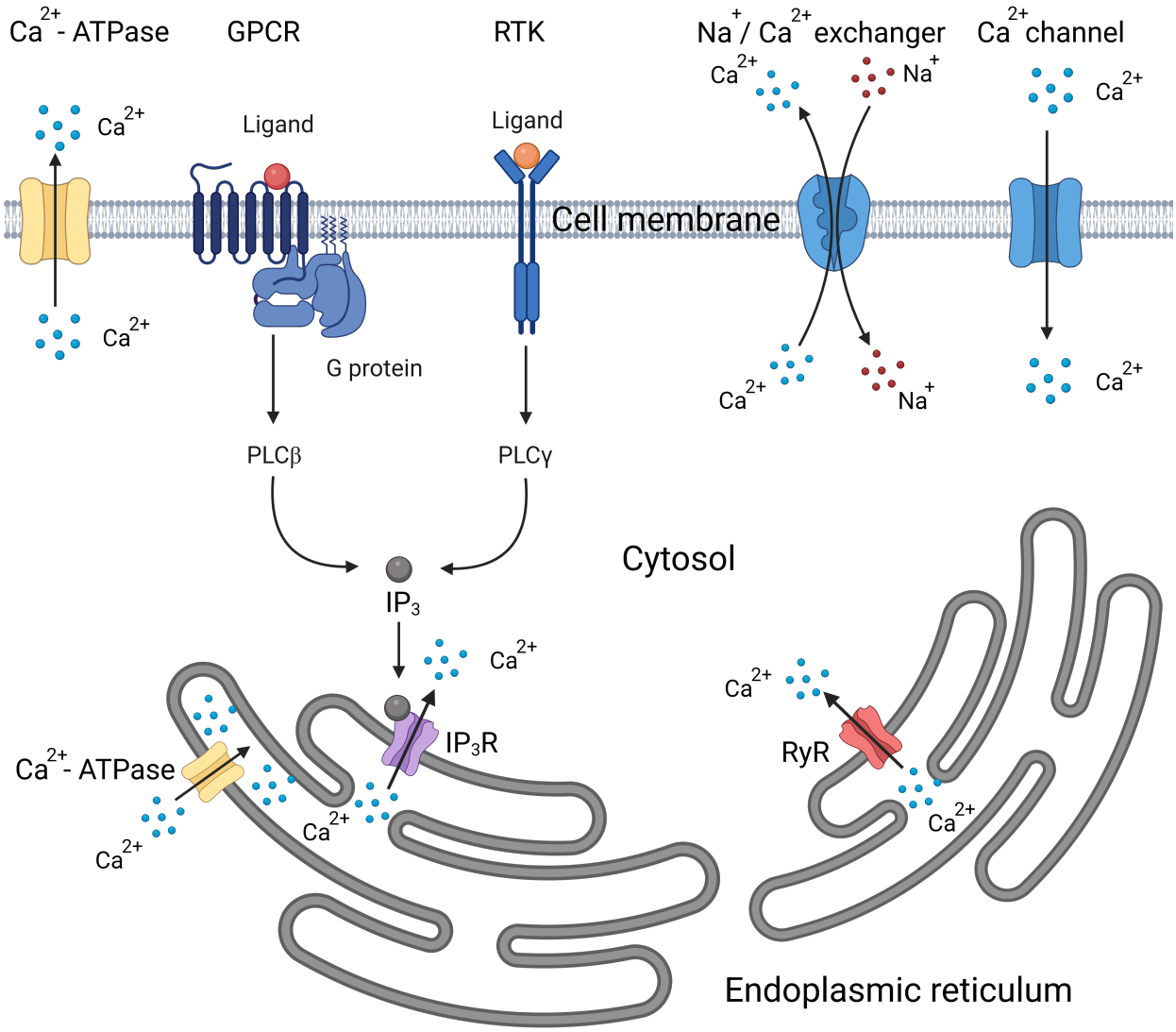

Fig. 2: An overview of intracellular Ca^{2+} regulation. The activation of GPCRs and RTKs on the cell membrane activates PLCβ and PLCγ respectively, resulting in the generation of IP_3. IP_3 binds to its receptor IP_3R on the membrane of the ER, releasing Ca^{2+} from the ER into the cytosol. Ca^{2+} can also enter the cytosol via Ca^{2+} channels on the cell membrane and RyRs on the ER. Excess Ca^{2+} is removed from the cytosol via Ca^{2+}-ATPases on the cell membrane and ER, and via Na^+/Ca^{2+} exchangers on the cell membrane. (Illustration by J. Lopez, created with BioRender)

1.3 Transient receptor potential channels (TRPs)

As mentioned in Chapter 1.2, Ca^{2+} can enter the cell from the extracellular space through TRPs located on the cell membrane. The TRP superfamily comprises cation

channels which vary in their degree of selectivity and mode of activation (27). TRPs are organised into homomers or heteromers consisting of 4 subunits with 6 transmembrane segments each (28). They can be divided into 7 subfamilies based on their sequence homology and functional characteristics, namely TRP canonical (TRPC), TRP vanilloid (TRPV), TRP ankyrin (TRPA), TRP melastatin (TRPM), no mechanopotential TRP (TRPN), TRP polycystic (TRPP) and TRP mucolipin (TRPML) channels (27) (see Fig. 3).

TRPs can be activated by a range of stimuli, which cause them to become more permeable to cations. TRPV1 (vanilloid receptor 1, capsaicin receptor), for example, can be stimulated by capsaicin (CAP), the chemical compound in chilli peppers responsible for its 'spicy' taste (29). They can also be stimulated by heat above 43°C, hypertonicity and acidic conditions (30, 31). These channels are classically found in nociceptors, which enable the sensory detection of noxious stimuli. Upon activation, TRPV1 allows an influx of cations into the cell which leads to a depolarisation of the cell membrane. When a threshold voltage is achieved, an action potential is generated and subsequently propagated along the neuron to the central nervous system where the signal is interpreted as pain (32).

Apart from their presence in neurons, TRPs are also expressed in non-excitable cells such as HCEC (28). The TRPs which have been identified in HCEC thus far are TRPC1, TRPC3, TRPC4, TRPV1, TRPV3, TRPV4 and TRPM8 (23, 33-37). These TRPs are crucial in the intracellular regulation of cations and play unique roles in the function of the cornea. The activation of TRPV1 for instance, is thought to be associated with inflammatory responses (34). TRPV1-4 are involved in heat detection (23), while TRPM8 activity exhibits an inhibitory effect on TRPV1 (37) in these cells. TRPC4 activity, on the other hand, has been shown to affect capacitative Ca^{2+} entry (CCE) in HCEC (33).

TRPs have also been identified in other parts of the eye, such as TRPM8, TRPV1, TRPV2 and TRPV4 in the conjunctiva (38, 39), TRPV1-3 and TRPM8 in the corneal endothelium (40, 41) as well as TRPV1 and TRPM8 in corneal keratocytes (42). Given the ubiquity of TRP channel expression in ocular cells and its significance in Ca^{2+}

regulation, it would be useful to study the activation mechanisms of these channels and the downstream pathways triggered by them. This would enable a better understanding of many intracellular processes which are regulated by TRPs and could facilitate the development of targeted treatments for ocular pathologies.

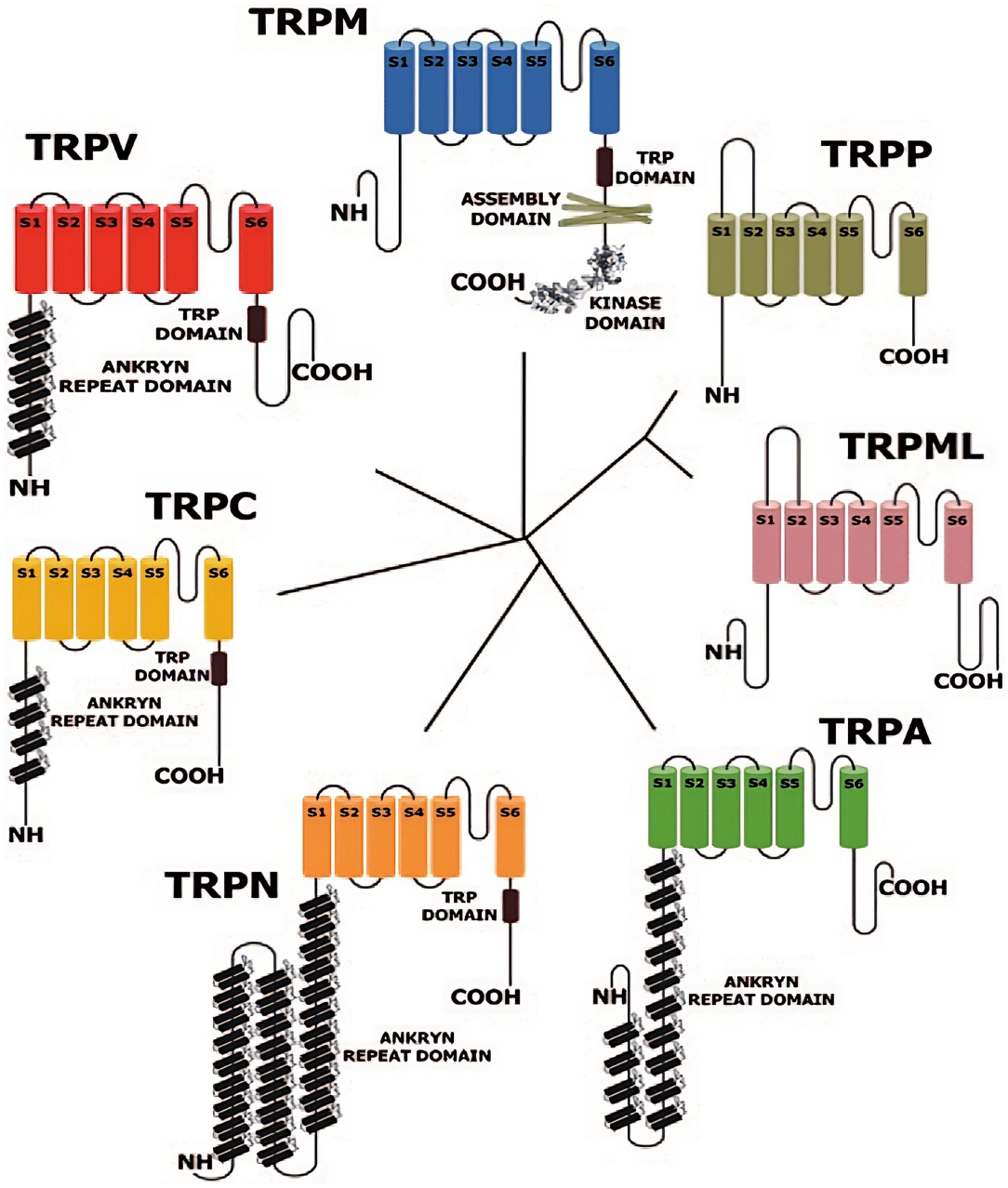

Fig. 3: The 7 TRP subfamilies and their structures. Each TRP channel subunit contains 6 transmembrane segments (S1–S6). TRPV, TRPC, TRPN and TRPA channels contain a variable number of ankyrin domains at the N-terminal regions. The TRP domain and protein

kinase domain can be found at the C-terminal regions of some TRPs. (Illustration by Ferreira et al., 2015 (43), reused with the kind permission of © Springer International Publishing)

1.4 Epidermal growth factor (EGF)

Epidermal growth factor (EGF) is a protein consisting of 53 amino acid residues (44) and is found in many different tissues in humans as well as other species. Binding of this protein to the EGF receptor (EGFR) induces a conformational change and subsequent dimerisation of the receptor. In its commonly known function, the EGFR then activates the intracellular tyrosine kinase domain of the receptor, which in turn triggers signal transduction cascades such as the JAK/STAT, PI3K/Akt and RAS/RAF/MEK pathways, ultimately promoting cellular differentiation and proliferation (45, 46) (see Fig. 4).

Accordingly, application of EGF has been shown to promote wound healing in the corneal epithelium. In a randomised controlled trial, patients with traumatic corneal epithelial defects recovered faster when they were treated with EGF compared to those who received a placebo (47). At the cellular level, application of EGF is known to stimulate proliferation and inhibit apoptosis of cultured HCEC (48). This can be attributed to the presence of EGFR, which is highly expressed in HCEC. In immortalised HCEC, the density of EGFR is reported to be approximately 1,300,000 receptors/cell. This is significantly higher than the expression of EGFR reported in any other physiological human cell type (49). For comparison, EGFR density in other tissue expressed as receptors/cell is approximately 200,000 in oral mucosa (50), 40,000 in corneal endothelium (51) and 24,000 in gastric smooth muscle (52). Immunofluorescence studies have shown that EGFR in HCEC is primarily found on the cell membranes in healthy corneal epithelium but tend to migrate towards intracellular regions when the epithelium is wounded (53). These characteristics suggest the importance of EGF signaling in HCEC and its significance in wound healing in the corneal epithelium. EGF would therefore be an ideal growth factor to test on HCEC due to the abundant availability of its receptor and its potential use in the treatment of corneal epithelial defects.

In previous studies, growth factors have also been shown to have specific effects on Ca^{2+} regulation in ocular tissue. For example, vascular endothelial growth factor (VEGF) was found to stimulate Ca^{2+} influx via TRPV1 in human corneal keratocytes (HCK) (42), while in rabbit corneal epithelial cells (RCEC), EGF caused intracellular Ca^{2+} store depletion and CCE via store-operated channels (SOCs) (54). Interactions between EGFR and members of the TRPC subfamily have also been demonstrated in various cell types before. One study was able to measure EGF-induced currents in HCEC, which were suppressed when TRPC4 was knocked down (33). This shows a link between EGFR and TRPC4 activity in HCEC, though the nature of this relationship remains poorly understood. In fibroblast-like cells, stimulation of the EGFR was found to cause tyrosine phosphorylation in TRPC4 (55) and TRPC6 (56), while in non-small cell lung carcinoma (NSCLC) cells, EGFR activation resulted in Ca^{2+} transients via TRPC1 (57). EGF is also able to activate murine TRPC4 and TRPC5 in transfected human embryonic kidney 293 cells (HEK-293) (58).

As evident from the research, it is not uncommon to find TRPs implicated in signaling pathways induced by growth factors like EGF. This means that EGF can affect a host of cellular processes not just via the conventional phosphorylation cascades, but also by influencing Ca^{2+} regulation in the cell. Research into the interplay between EGFR and TRPs could enhance our understanding of the effects growth factors have on the cell and how these effects can be modified with specific TRP channel modulators. To gain a better idea of how growth factors affect Ca^{2+} regulation in the corneal epithelium, this study will investigate the relationship between EGF and TRPs in HCEC.

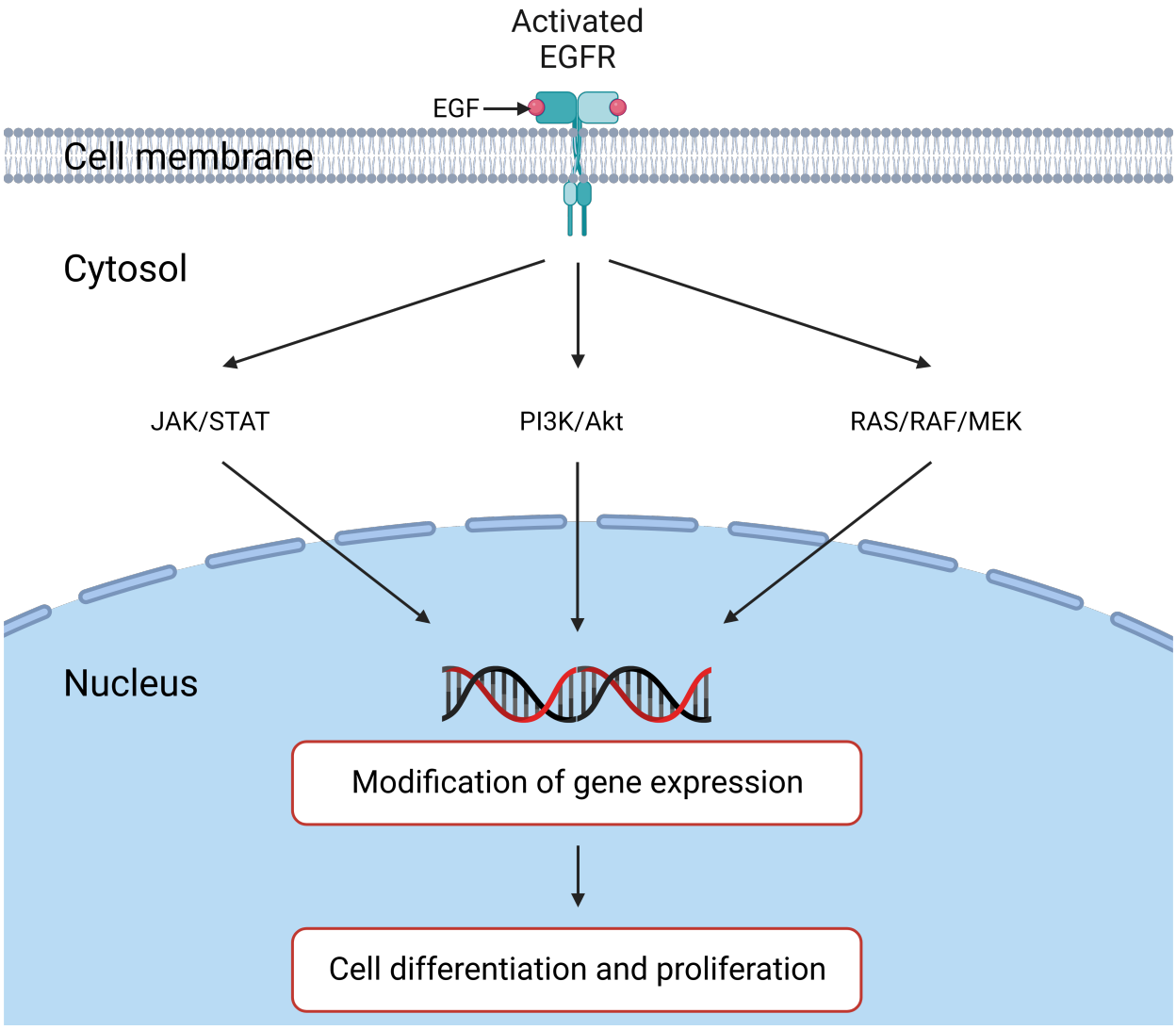

Fig. 4: The EGF signaling pathway. Binding of EGF activates the EGFR on the cell membrane, triggering the JAK/STAT, PI3K/Akt and RAS/RAF/MEK pathways within the cell. This results in an altered expression of genes, promoting cellular differentiation and proliferation. (Illustration by J. Lopez, created with BioRender)

1.5 Aim of study

Given that a functional corneal epithelium is necessary for maintaining normal vision, research should be conducted into the methods which promote healing of this layer to benefit patients with a damaged cornea. While the use of EGF has shown promising results in this regard, its mechanism of action, particularly in connection with TRPs, is

not fully understood. In view of the current understanding of electrophysiological characteristics of HCEC and the techniques available to observe them, the following objectives were defined (see Fig. 5):

- To characterise the effect of EGF on Ca^{2+} regulation in HCEC. In particular, it will be investigated if TRPs can be activated by external application of EGF. The corresponding activity of TRPs will be measured using fluorescence Ca^{2+} imaging.
- To determine the subtype of TRPs involved in the EGF-induced effect on HCEC using well-established TRP channel antagonists. Two of such antagonists are BCTC, which is an antagonist of TRPM8 and TRPV1, and SKF 96365, which is an antagonist of TRPC channels.
- To ascertain if intracellular Ca^{2+}-release channel activity contributes to the effect induced by EGF in HCEC. This will be done by comparing the changes in intracellular Ca^{2+} upon application of EGF to HCEC in Ca^{2+}-free and Ca^{2+}-containing measuring solutions.
- To verify the involvement of TRPs on the cell membrane by conducting whole-cell patch-clamp recordings of HCEC in the presence of EGF. If an increase in whole-cell currents is detected, the effect will be tested again in the presence of the TRP channel antagonist previously shown to be effective in suppressing the EGF effect.

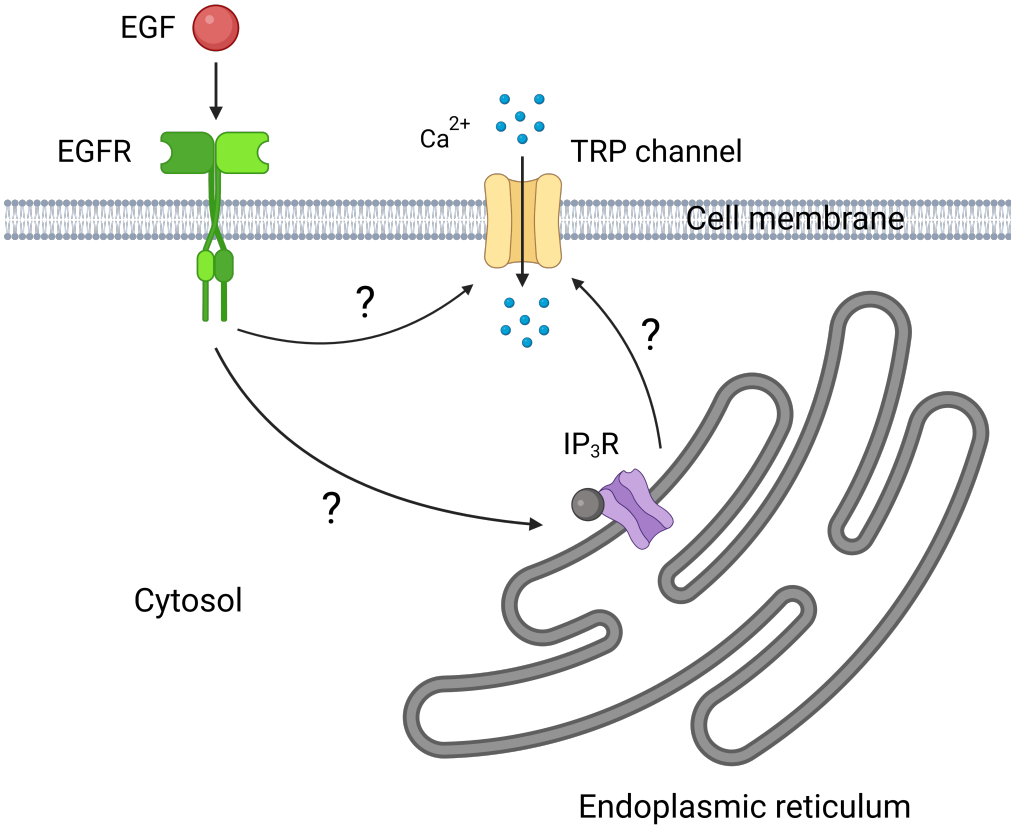

Fig. 5: A schematic representation of the aims of this study. The first objective is to determine if there is a relationship between activation of the EGFR and TRP channel activity in HCEC. TRP channel antagonists will then be used to ascertain the type of TRP channel involved. Once the type of channel has been established, the possible contribution of intracellular Ca^{2+}-release channels to the EGF effect will be investigated. One such channel is the IP_3R found on the ER, which may contribute to an activation of SOCs on the cell membrane and lead to an intracellular Ca^{2+} increase. Lastly, patch-clamp whole-cell currents will be measured to confirm if EGF induces activation of TRPs on the cell membrane. (Illustration by J. Lopez, created with BioRender)

2 Methods

2.1 Chemicals and solutions

Ringer-like solution

A Ringer-like solution was used to form test solutions for fluorescence Ca^{2+} imaging experiments, as well as to provide an aqueous medium for cells observed under the fluorescence microscope.

Two types of Ringer-like solution were used, depending on the experiment being conducted.

In one series of experiments, the Ringer-like solution consisted of 150 mM NaCl, 1.5 mM $CaCl_2$, 6 mM CsCl, 1 mM $MgCl_2$, 10 mM glucose and 10 mM HEPES buffer at pH 7.4.

In experiments where Ca^{2+}-free conditions were required, a different composition was used, containing 150 mM NaCl, 6 mM CsCl, 1 mM $MgCl_2$, 1 mM EGTA and 10 mM HEPES-acid at pH 7.4.

EGF

50 ng/ml EGF from Thermo Fisher Scientific (Karlsruhe, Germany) was tested on HCEC in both the patch-clamp as well as fluorescence Ca^{2+} imaging experiments.

SKF 96365

10 µM and 20 µM of SKF 96365 were used in fluorescence Ca^{2+} imaging experiments and 20 µM was used in the patch-clamp experiments. This TRPC channel antagonist was obtained from Sigma-Aldrich (Deisenhofen, Germany).

BCTC

10 µM of the TRPM8/TRPV1 antagonist BCTC was used in fluorescence Ca^{2+} imaging experiments. This was obtained from Tocris Bioscience (Bristol, UK).

Fura-2AM

The Ca^{2+}-sensitive fluorescent dye Fura-2AM used in fluorescence Ca^{2+} imaging experiments was obtained from Tocris Bioscience (Bristol, UK). 2–3 µM was used to dye the cells.

Culture medium

Dulbecco's Modified Eagle Medium (DMEM) and Ham's F-12 used in the culture medium for the cells were obtained from Thermo Fisher Scientific (Karlsruhe, Germany) or Biochrom GmbH (Berlin, Germany).

Antibiotics

The antibiotics penicillin and streptomycin used for cell cultivation were obtained from Thermo Fisher Scientific (Karlsruhe, Germany).

Accutase solution

Accutase solution was used to detach cells from the surface of the culture flasks. This was obtained from Thermo Fisher Scientific (Karlsruhe, Germany).

Phosphate buffered saline (PBS)

Mg^{2+}- and Ca^{2+}-free PBS solution from Thermo Fisher Scientific (Karlsruhe, Germany) was used to wash the cells.

Fetal calf serum (FCS)

Medium containing FCS was added to stop the effect of Accutase. This serum was obtained from Thermo Fisher Scientific (Karlsruhe, Germany).

Patch-clamp external solution

1 ml of an external solution from Nanion Technologies (Munich, Germany) was used to create the cell suspension for patch-clamp experiments. 5 µl of the external solution was also added to the external side of the microchip in the patch-clamp setup before addition of the cell suspension. It consisted of 2 mM $CaCl_2$, 4 mM KCl, 1 mM $MgCl_2$, 140

mM NaCl, 5 mM D-glucose monohydrate and 10 mM HEPES buffer with NaOH at a pH of 7.4 and osmolarity of 298 mOsmol. A seal enhancing solution was used temporarily to improve the seal quality. It consisted of 80 mM NaCl, 3 mM KCl, 10 mM $MgCl_2$, 35 mM $CaCl_2$, 10 mM HEPES (Na^+-salt)/HCl at a pH of 7.4 and osmolarity of 298 mOsmol.

Patch-clamp internal solution

5 µl of an internal solution from Nanion Technologies (Munich, Germany) was added to the internal side of the microchip in the patch-clamp setup. It consisted of 50 mM CsCl, 10 mM NaCl, 60 mM CsF, 20 mM EGTA and 10 mM HEPES buffer with KOH at a pH of 7.2 and osmolarity of 288 mOsmol. CsCl was included to suppress outward rectifying K^+ currents.

2.2 Cultivation of HCEC

The cell line used in the experiments was established by Araki-Sasaki et al. (59), where corneal epithelial cells were isolated from a cornea of a 49-year-old woman with maxillary sinus carcinoma then immortalised with a recombinant SV-40-adenovirus vector. The SV40-adenovirus immortalised HCEC were kindly provided by Friedrich Paulsen (Institute of Anatomy, University of Nuremberg, Germany). The cells were grown in a 1:1 mixture of DMEM and Ham's F-12, supplemented with 10% FCS and antibiotics (penicillin and streptomycin) in a humidified 5% CO_2 incubator at 37°C.

The cell cultivation process is described as follows. The cells were initially washed twice with 10 ml Mg^{2+}- and Ca^{2+}-free PBS solution in a T25 flask, after which 2 ml Accutase was added to dissociate the cells from the flask. This mixture was incubated at 37°C and 5% CO_2 for approx. 3–5 minutes. 10 ml of medium containing FCS was then added to stop the activity of Accutase and the cells were carefully mixed with a pipette to prevent clumping. The resultant mixture was centrifuged at a relative centrifugal force (RCF) of 800 (≈ 100 × g) for 5 minutes to separate the cells, which were then removed and resuspended in 10 ml of medium with FCS and incubated at 37°C with 95% H_2O and 5% CO_2 for 1–5 days before the measurements were conducted.

2.3 Fluorescence Ca^{2+} imaging

A fluorescence imaging system (Olympus, Hamburg, Germany) was used to detect and quantify very small changes in intracellular Ca^{2+} concentration in HCEC while the cells were exposed to different test solutions (see Fig. 6).

Coverslips containing the cells were first incubated with 2–3 μM of a Ca^{2+}-sensitive fluorescent dye Fura-2AM for about 30–40 minutes with 5% CO_2 at 37°C in the dark. Fura-2AM binds Ca^{2+} ions and the intensity of its fluorescence varies with the concentration of Ca^{2+} and the excitation wavelength of UV light it is exposed to. The fluorescence intensity of Fura-2-AM increases with increasing Ca^{2+} concentration when exposed to UV light at 340 nm and decreases with increasing Ca^{2+} concentration when exposed to UV light at 380 nm. The properties of Fura-2AM are explored in greater detail in Grynkiewicz et al. (60) In instances where a TRP channel antagonist was required, the antagonist was added to the cells in the concentration being tested, along with Fura-2AM.

After incubation, the coverslips with the stained cells were immersed in the Ringer-like solution described in Chapter 2.1 to remove excess dye and cell debris, then loaded onto the bath chamber on the object table of the fluorescence microscope. 2 ml of fresh Ringer-like solution was also added to provide an aqueous medium for the cells. In experiments where a channel antagonist was required, it was present in the Ringer-like solution and all test solutions used, in the concentration being tested. Using cellSens Life Science Imaging Software (Olympus, Hamburg, Germany), individual cells were marked out as regions of interest (61) for measurement (see Fig. 7). An automated process was then started, whereby UV light at 2 different excitation wavelengths – 340 nm and 380 nm – were directed alternately at the cells at regular intervals and the corresponding intensity of fluorescence at a wavelength of 510 nm (green light) emitted by Fura-2AM was measured. This was recorded as fluorescence ratio f_{340}/f_{380} – the ratio of intensity of fluorescence emitted in response to excitation wavelength 340 nm to that of excitation wavelength 380 nm – and plotted against time. At predetermined points of time during the process, 2 ml of test solution was pipetted to the cells while the existing solution was washed out with a pump.

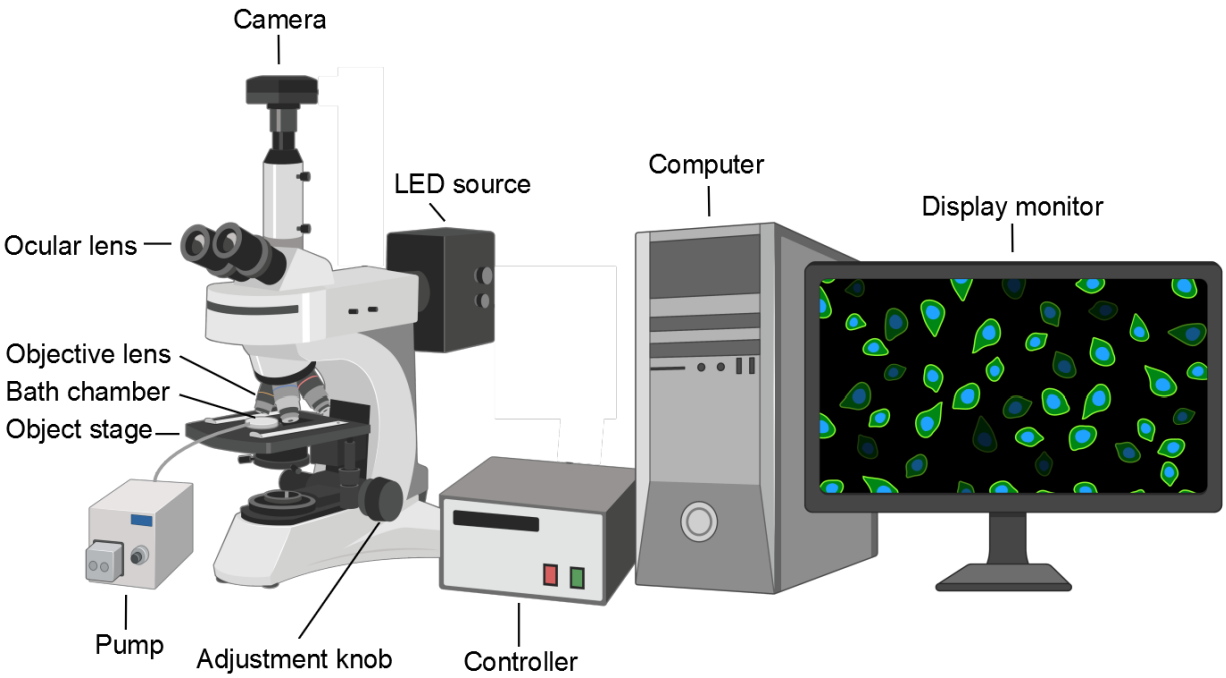

Fig. 6: A simplified schematic of the fluorescence imaging system used for Ca^{2+} measurements. Cells and test solutions were loaded onto a bath chamber located on the object stage. When a change in test solution was required, the existing solution was washed out from the bath chamber with a pump. An LED source was connected to a computer via a controller to control the duration of light exposure to the cells, while the objective and ocular lenses magnified the image. A digital camera captured the magnified images and transmitted them to the computer to be processed. The cells could be viewed either through the ocular lens of the microscope or on the computer's display monitor. (Illustration by J. Lopez, created with Biorender)

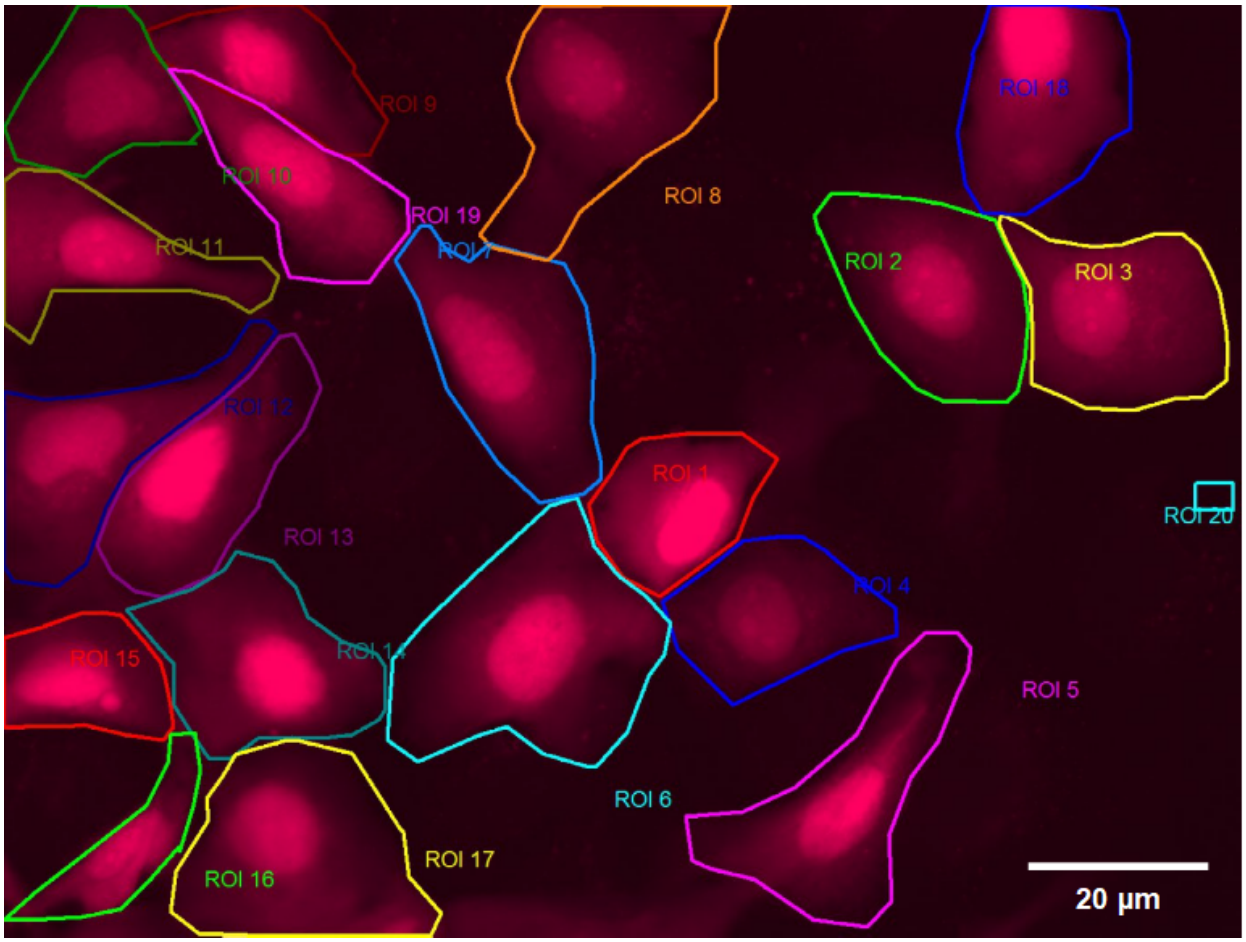

Fig. 7: HCEC incubated with Fura-2AM viewed under a fluorescence microscope. The cells emitted a green fluorescence but were displayed in red by the imaging software. Individual cells were marked out as regions of interest (ROI) then observed for changes in fluorescence when exposed to different test solutions at specific points of time. ROI 20 (light blue rectangle on the right) is a region without any cells and was designated as the ROI for background fluorescence. This enabled a clearer distinction to be made between cell fluorescence and any background fluorescence during measurements and increased the signal-to-noise ratio. (Photo by J. Lopez)

2.4 Planar patch-clamp technique

The planar patch-clamp technique allows measurement of very small ionic currents across a cell membrane. In this study, the Port-a-Patch system (Nanion Technologies, Munich, Germany) was used to measure whole-cell currents in HCEC when exposed to different test solutions (see Fig. 8).

The HCEC to be tested were prepared in same manner as cell culture described in Chapter 2.2. However, after centrifugation, they were resuspended in the external solution instead of the culture medium and FCS. The cells were then manually mixed with a pipette to obtain a single-cell suspension and analysed under a microscope.

Before beginning the measurements, the electrodes were chlorided. 5 µl of internal solution was pipetted onto the underside of a microchip which was then screwed onto the chip holder. The shielding was replaced and 5 µl of external solution was added to the top of the microchip, followed by 5 µl of the HCEC suspension. A software-controlled pump was then used to create a seal between a single cell and the microchip.

Using the acquisition software PatchMaster (HEKA Elektronik, Lambrecht, Germany), the seal resistance was optimised by adjusting factors such as the suction pressure of the pump. Once a stable seal was achieved, a voltage stimulation protocol was started. Whole-cell currents were measured for 500 ms every 5 s over a voltage range of −60 mV to +130 mV (ramp protocol). The current densities (pA/pF) were calculated as the ratio of the current (pA) to the cell membrane capacitance (pF). At predetermined points of time during the recording (usually 2 or 4 minutes), test solutions were applied to the cell. This was done by pipetting 5 µl of the test solution to the top of the microchip and removing 5 µl of the resulting mixture, then repeating this twice more.

The liquid junction potential was software calculated and accounted for (62). The mean membrane capacitance of 8.9 ± 0.4 pF (n = 4) and mean access resistance of 11.2 ± 2.0 MΩ (n = 4) were also software calculated. The series resistance (Rs) as well as fast and slow capacitance transients were compensated for using a patch-clamp amplifier controlled by PatchMaster. The measured whole-cell currents were leak-subtracted and cells with leak currents above 100 pA were excluded from the analysis. All measurements were conducted at room temperature of approximately 22°C. The holding potential (HP) was set to 0 mV in order to prevent measurement errors due to the activity of voltage-dependent Ca^{2+} channels (VDCCs).

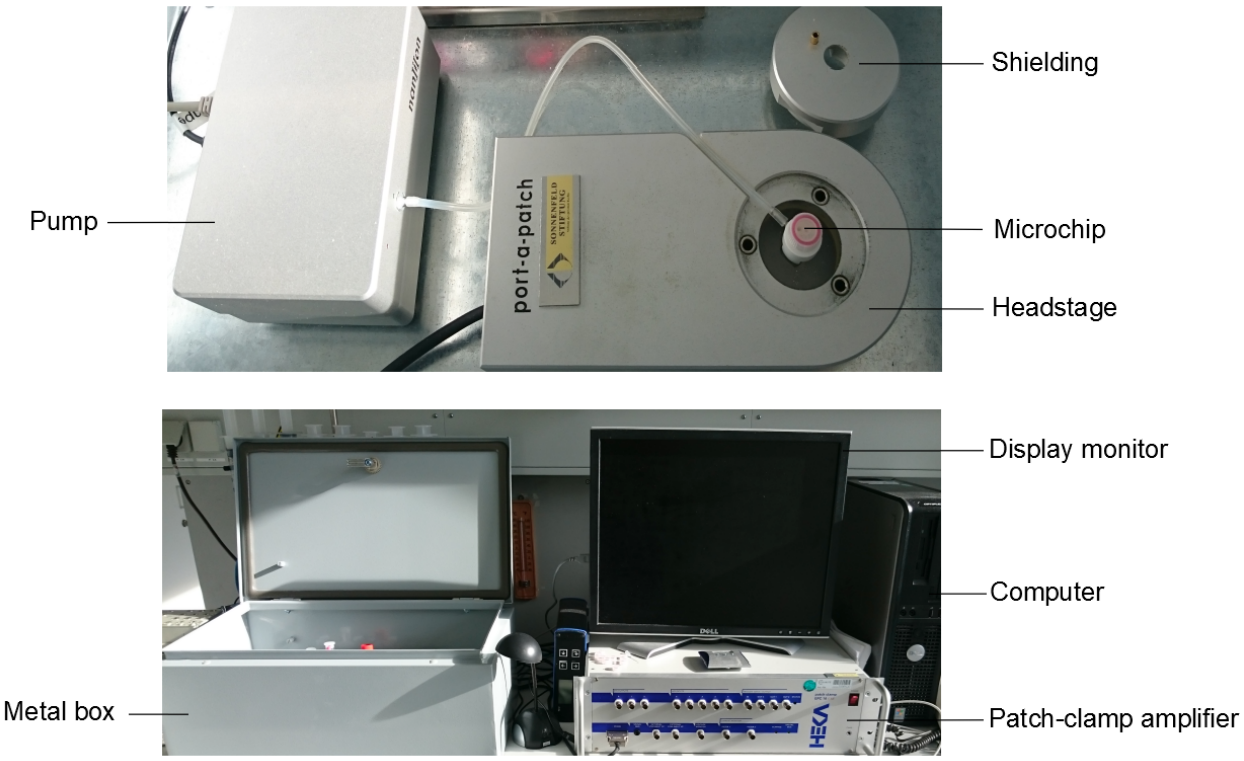

Fig. 8: Planar patch-clamp setup used for measuring current flow across the cell membrane. During the experiments, the microchip which contained the cells and test solutions was fixed onto the headstage and covered with the shielding. The pump exerted a suction pressure to create a seal between a single cell and the microchip. The headstage transmitted electrical signals from the microchip to the amplifier, which measured these currents and sent the data to a computer to be analysed. The sensitive electrical components of the setup were kept in a metal box, which functioned as a Faraday cage. This was to prevent any external electrical fields from interfering with the measurements of very small currents. (Photos by J. Lopez)

2.5 Statistical analysis

Several statistical tests were conducted to determine if there were significant differences between data sets obtained from the experiments. All significance tests were two-tailed and the results were deemed significant if the p-value was less than 5%. Results are shown as mean values ± standard error of mean (SEM). Normality was tested for using the Kolmogorov-Smirnov test, the D'Agostino & Pearson normality test and the Shapiro-Wilk normality test.

For comparison of data sets before and after addition of test solutions to the same cell or group of cells, a paired Student's t-test was conducted if the data followed a Gaussian distribution, and a non-parametric Wilcoxon signed-rank test was used if they did not.

When comparing data sets of different cells or groups of cells, for example the effect of a test solution with that of a control, an unpaired Student's t-test was used if the data followed a Gaussian distribution, and a non-parametric Mann-Whitney U test was used if they did not.

Plotting of graphs and statistical evaluation of the data were done with SigmaPlot (Systat Software, San Jose, California, USA) and GraphPad Prism (GraphPad Software, San Diego, California, USA).

2.6 Guidelines

All experiments performed in this study are in accordance with the ethical guidelines "Grundsätze der Charité Universitätsmedizin Berlin zur Sicherung guter wissenschaftlicher Praxis" (20.06.2012). As the experiments were conducted *in vitro* on cultured cells from an established cell line, approval by an ethics committee was not required. The data acquired from the experiments are stored on servers of the Charité and locally in the Department of Ophthalmology, Charité Campus Virchow-Klinikum, Berlin.

3 Results

3.1 HCEC morphology

The morphological characteristics of cultured HCEC were observed under a light microscope at a magnification of 20×10. The cells showed a spindle form with a centrally located nucleus and tended to grow in close proximity, forming cell clusters of varying sizes (see Fig. 9).

HCEC cultures which were cultured over a longer period of time showed a higher number of cell clusters and a greater cell density in each cluster. However, when cell density was too high, the cells began to lose their physiological characteristics. This was evident from the irregular shapes observed under a standard light microscope.

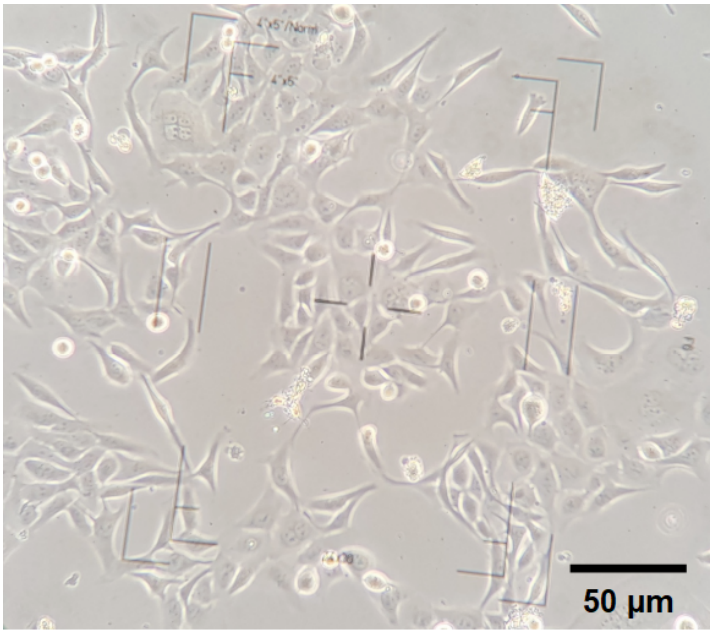

Fig. 9: Cultured HCEC seen under a light microscope at 20×10 magnification. The cells display a typical spindle form and grow in clusters. (Photo kindly provided by S. Mergler)

3.2 EGF induces intracellular Ca^{2+} increase in HCEC via TRPC channels

To determine the effect of EGF on intracellular Ca^{2+} concentration in HCEC, 50 ng/ml EGF was added extracellularly to the cells after the 4^{th} minute in a 10-minute experiment. This caused a significant increase in fluorescence ratio (f_{340}/f_{380}), which

corresponds to an increase in intracellular Ca^{2+} concentration. The fluorescence ratio increased from 0.1008 ± 0.0004 at 100 s (control) to 0.1259 ± 0.0027 at 600 s in the presence of EGF (mean ± SEM; n = 85, $p < 0.0001$) (see Fig. 10 A and B).

The experiment was then repeated in the presence of the TRPM8/TRPV1 antagonist BCTC. The effect caused by 50 ng/ml EGF was not reduced in the presence of 10 µM BCTC. A similar increase in intracellular Ca^{2+} concentration was observed upon the addition of EGF, indicating that neither TRPM8 nor TRPV1 were involved in the EGF-induced Ca^{2+} increase (see Fig. 11).

Next, the experiments were conducted in the presence of the TRPC channel antagonist SKF 96365.

In the presence of 10 µM of SKF 96365, a partial suppression of the EGF effect was observed, indicating an involvement of TRPC channels in the EGF effect. The fluorescence ratio increased slightly from 0.1000 ± 0.0004 at 100 s (control) to 0.1067 ± 0.0007 at 600 s in the presence of EGF and SKF 96365 (mean ± SEM; n = 40, $p < 0.0001$) (see Fig. 12 A). This increase was significantly smaller than that without the antagonist ($p < 0.0001$) (see Fig. 12 C).

In the presence of a higher concentration of SKF 96365 (20 µM), a complete suppression of the EGF effect was observed, showing a dose-dependent inhibition of the EGF effect by the antagonist. There was no significant increase in intracellular Ca^{2+} concentration after addition of EGF. The fluorescence ratio was 0.1011 ± 0.0004 at 100 s (control) and 0.1022 ± 0.0008 at 600 s in the presence of EGF and SKF 96365 (mean ± SEM; n = 75, $p = 0.1691$) (see Fig. 12 B).

In summary, the results indicate that the EGF-induced Ca^{2+} increase in HCEC was due to TRPC channel activation, since the corresponding TRPC channel antagonist clearly suppressed this effect. Moreover, a significantly stronger suppression of the EGF-induced Ca^{2+} increase was observed in the presence of the higher concentration compared to the lower concentration of SKF 96365 ($p = 0.0003$) (see Fig. 12 C).

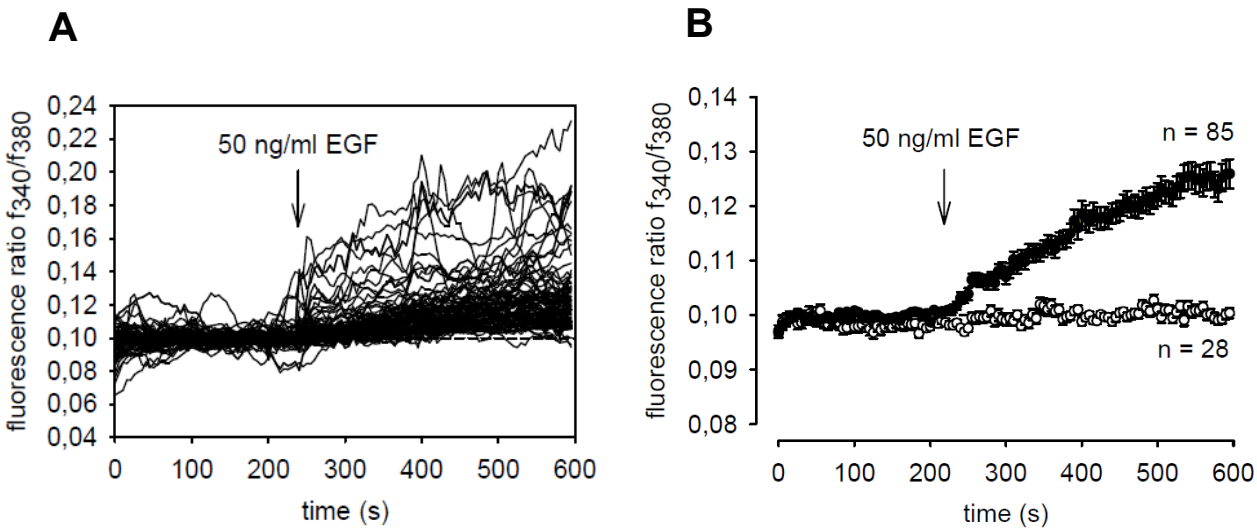

Fig. 10: Changes in fluorescence ratios (f_{340}/f_{380}) of HCEC when exposed to 50 ng/ml EGF. The arrows represent the point in time where EGF was added to the cells. (**A**) shows the fluorescence ratios of 85 individual cells exposed to 50 ng/ml EGF after the 4th minute. In (**B**), the filled circles represent the mean fluorescence ratios of HCEC being tested (n = 85) and the open circles form a baseline representing the mean fluorescence ratios of HCEC without any EGF exposure (n = 28).

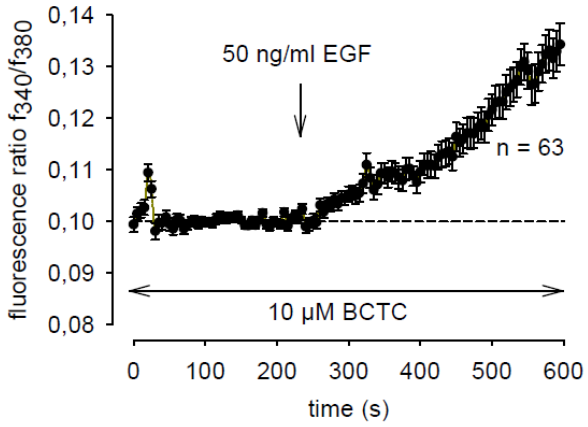

Fig. 11: Mean fluorescence ratios (f_{340}/f_{380}) of HCEC when exposed to 50 ng/ml EGF in the presence of 10 µM BCTC (n = 63). EGF was added to the cells at the 4th minute while BCTC was present throughout the experiment, as indicated by arrows respectively. The fluorescence signal increased after application of EGF, despite the presence of the TRPM8/TRPV1 antagonist.

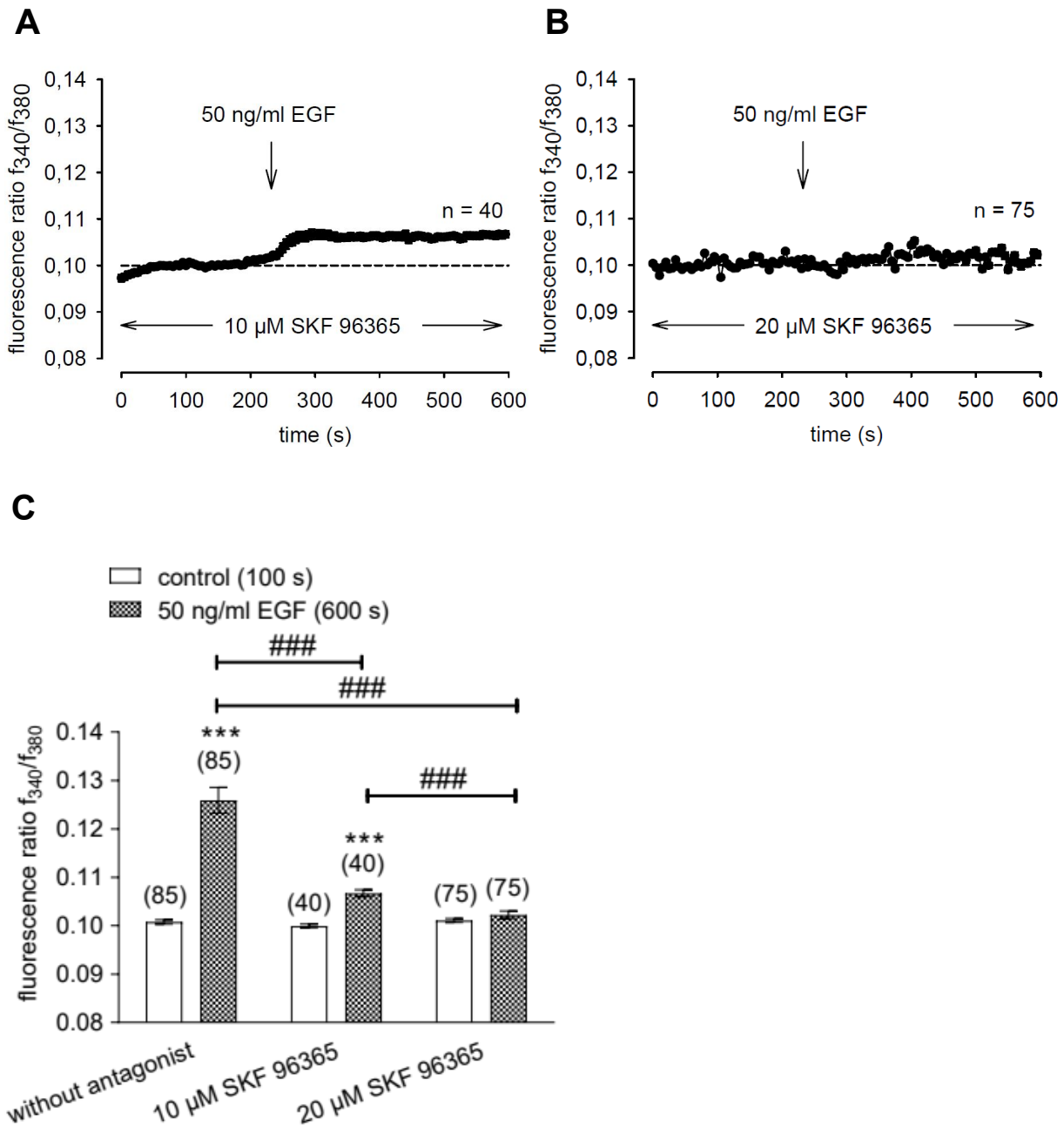

Fig. 12: Comparison of mean fluorescence ratios (f_{340}/f_{380}) of HCEC when exposed to 50 ng/ml EGF in the presence of different concentrations of SKF 96365. (**A**) and (**B**) show the mean fluorescence ratios of HCEC exposed to 50 ng/ml EGF after the 4th minute in the presence of 10 µM SKF 96365 (n = 40) and 20 µM (n = 75) SKF 96365 respectively. The downward arrows represent the point in time where EGF was added to the cells. (**C**) compares the change in mean fluorescence ratios of HCEC before and after addition of 50 ng/ml EGF under three different conditions; without a TRP channel antagonist (n = 85), with 10 µM SKF 96365 (n = 40)

and with 20 µM SKF 96365 (n = 75). The asterisks (*) designate significant differences between the mean fluorescence ratios of HCEC before and after addition of EGF, the hashes (#) designate significant differences between the EGF-induced effect with different concentrations of SKF 96365 used.

3.3 The EGF effect on HCEC in the presence and absence of extracellular Ca^{2+}

The next experiment was conducted to investigate if extracellular Ca^{2+} was necessary for the EGF-induced Ca^{2+} increase in HCEC. At the start of the measurements, the cells were exposed to 1.5 mM Ca^{2+}-containing Ringer-like solution. After the 4th minute, this Ringer-like solution was replaced with 1 mM EGTA Ca^{2+}-free Ringer-like solution, whereby a corresponding decrease in intracellular Ca^{2+} concentration was observed. The fluorescence ratio decreased significantly from 0.0996 ± 0.0003 at 100 s (control) to 0.0706 ± 0.0025 at 400 s in the Ca^{2+}-free solution (mean ± SEM; n = 73, $p < 0.0001$). Subsequently, 50 ng/ml EGF in a Ca^{2+}-free solution was added to the cells after the 8th minute. This caused no increase in the intracellular Ca^{2+} concentration, indicating that extracellular Ca^{2+} was necessary for the EGF-induced Ca^{2+} increase. The fluorescence ratio continued to decrease significantly from 0.0706 ± 0.0025 at 400s in the Ca^{2+}-free solution to 0.0604 ± 0.0033 at 900 s in the Ca^{2+}-free solution with EGF (mean ± SEM; n = 73, $p < 0.0001$) (see Fig. 13 A and B). EGF therefore did not elicit a response in HCEC the absence of extracellular Ca^{2+}.

The same experiment was then repeated, but this time, 1.5 mM Ca^{2+}-containing Ringer-like solution was added back extracellularly together with 50 ng/ml EGF to the cells after the 8th minute. This time, significant increase in intracellular Ca^{2+} concentration above the baseline was observed after the addition of EGF, confirming that this EGF-induced Ca^{2+} increase could only occur in the presence of extracellular Ca^{2+}. The fluorescence ratio initially decreased significantly from 0.1013 ± 0.0005 at 100 s (control) to 0.0862 ± 0.0013 at 460 s in the Ca^{2+}-free solution (mean ± SEM; n = 69, $p < 0.0001$) and increased significantly to 0.1129 ± 0.0016 at 600 s in the Ca^{2+}-containing solution with EGF (mean ± SEM; n = 69, $p < 0.0001$) (see Fig. 13 C).

As a control to demonstrate the effect of returning extracellular Ca^{2+} alone on intracellular Ca^{2+} concentration of HCEC, another experiment was conducted where 1.5

mM Ca^{2+}-containing Ringer-like solution was replaced with 1 mM EGTA Ca^{2+}-free Ringer-like solution after the 4th minute, which was then replaced again with 1.5 mM Ca^{2+}-containing Ringer-like solution after the 8th minute. EGF was not added to the cells. The fluorescence ratio first decreased significantly after the 4th minute from 0.0991 ± 0.0008 at 100 s in the Ca^{2+}-containing solution to 0.0872 ± 0.0012 at 460 s in the Ca^{2+}-free solution (mean ± SEM; n = 19, p = 0.0001) and then increased significantly after the 8th minute to 0.0955 ± 0.0015 at 600 s in the Ca^{2+}-containing solution (mean ± SEM; n = 19, p < 0.0001). There was no significant difference in fluorescence ratios at 100 s (control) and at 600 s (n = 19, p = 0.0671), showing that the introduction of extracellular Ca^{2+} alone did not produce an intracellular Ca^{2+} increase beyond the baseline level in HCEC (see Fig. 13 D).

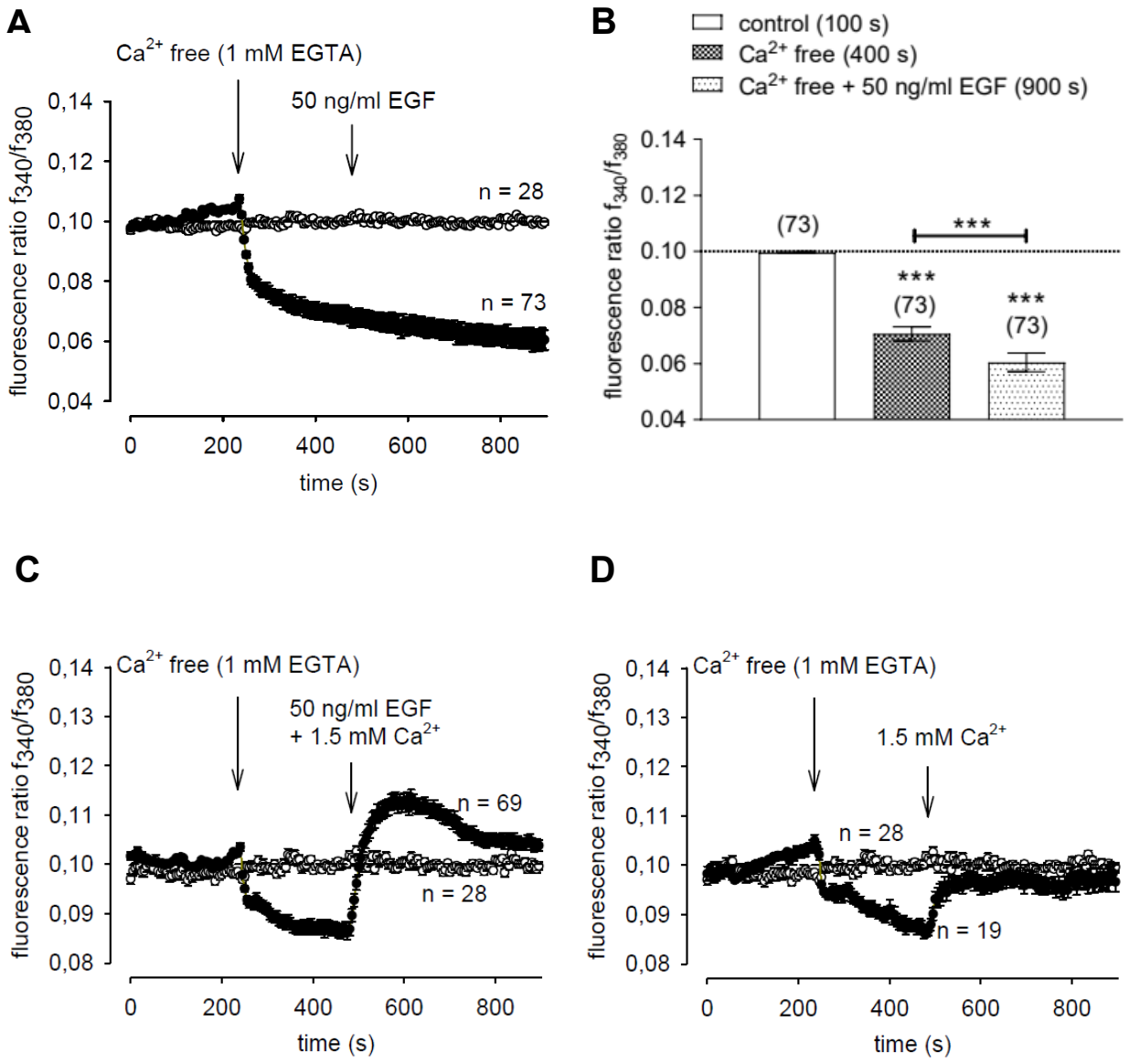

Fig. 13: Effect of 50 ng/ml EGF on mean fluorescence ratios (f_{340}/f_{380}) of HCEC in Ca^{2+}-containing and Ca^{2+}-free measuring solutions. The arrows represent the points in time where the respective solutions were added. In (**A**), the Ca^{2+}-containing measuring solution was replaced with a Ca^{2+}-free Ringer-like solution containing 1 mM EGTA after the 4th minute and 50 ng/ml EGF was added to the HCEC after the 8th minute. The filled circles represent the mean fluorescence ratios of HCEC being tested (n = 73) and the open circles form a baseline representing the mean fluorescence ratios of HCEC in Ca^{2+}-containing solution without any EGF exposure (n = 28). (**B**) compares the mean fluorescence ratios of HCEC in this experiment in three instances; in 1.5 mM Ca^{2+}-containing measuring solution, when Ca^{2+} is removed from the measuring solution and when 50 ng/ml EGF is subsequently added in the absence of

extracellular Ca^{2+} (n = 73). The asterisks (*) designate significant differences in the mean fluorescence ratios of HCEC at the different points in time. In (**C**), the same experiment was carried out but with 1.5 mM Ca^{2+} added back to the measuring solution together with 50 ng/ml EGF after the 8th minute. The filled circles represent the mean fluorescence ratios of HCEC being tested (n = 69) and the open circles form a baseline representing the mean fluorescence ratios of HCEC in Ca^{2+}-containing solution without any EGF exposure (n = 28). (**D**) shows the effect of merely removing Ca^{2+} from the measuring solution after the 4th minute and adding 1.5 mM Ca^{2+} back after the 8th minute, without application of EGF. The filled circles represent the mean fluorescence ratios of HCEC being tested (n = 19) and the open circles form a baseline representing the mean fluorescence ratios of HCEC in Ca^{2+}-containing solution (n = 28).

3.4 EGF induces whole-cell currents in HCEC

Planar patch-clamp experiments were also conducted on HCEC to detect changes in whole-cell currents across the cell membrane when the cells were exposed to EGF in the presence and absence of SKF 96365.

Whole-cell currents increased when 50 ng/ml EGF was added to the cells and decreased when 20 µM SKF 96365 was additionally present (see Fig. 14 A and B). At a stimulation voltage of -60 mV, inward currents increased significantly from -22.78 ± 6.94 pA/pF to -52.20 ± 16.39 pA/pF (mean ± SEM; n = 5, p = 0.0404) upon application of EGF and decreased significantly to -27.12 ± 10.70 pA/pF (mean ± SEM; n = 5, p = 0.0192) when SKF 96365 was additionally present. At a stimulation voltage of 130 mV, outward currents increased significantly from 186.70 ± 55.68 pA/pF to 266.40 ± 82.02 pA/pF (mean ± SEM; n = 5, p = 0.0410) upon application of EGF and decreased significantly to 176.10 ± 57.60 pA/pF (mean ± SEM; n = 5, p = 0.0231) when SKF 96365 was additionally present (see Fig. 14 C).

These observations suggest that the EGF-induced increase in inward and outward whole-cell currents in HCEC was due to TRPC channel activation, since the effect could be reduced in the presence of the TRPC channel antagonist SKF 96365.

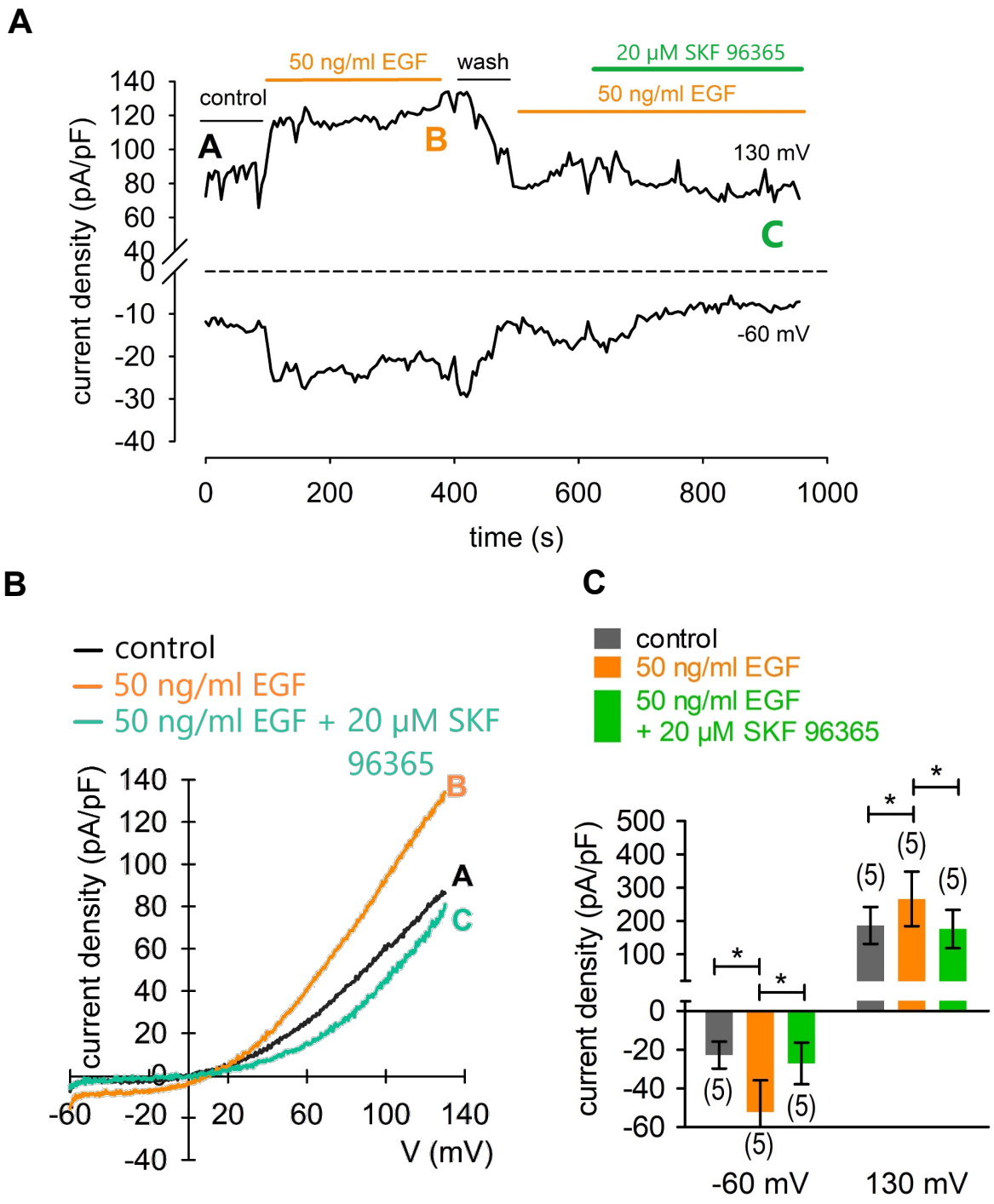

Fig. 14: Effect of 50 ng/ml EGF with and without 20 µM SKF 96365 on whole-cell currents in HCEC. **(A)** shows the time course recording of whole-cell currents at -60 mV (lower trace) and 130 mV (upper trace). The currents were normalised to cell membrane capacitance (current density; pA/pF). 50 ng/ml EGF led to a large increase in whole-cell currents, which decreased after washout of EGF (recovery). A second EGF application also increased whole-cell currents,

whereas application of 20 μM SKF 96365 suppressed this effect. In **(B)**, original traces reflect the change in whole-cell currents in response to voltage ramps. The traces show currents before application of test solutions (trace A), after application of 50 ng/ml EGF (trace B), and after application of 50 ng/ml EGF with 20 μM SKF 96365 (trace C). **(C)** shows the comparison of whole-cell current changes induced by 50 ng/ml EGF with and without 20 μM SKF 96365 at -60 mV and 130 mV. The asterisks (*) designate statistically significant differences in whole-cell currents.

4 Discussion

4.1 Involvement of TRPC channels in EGF-induced Ca^{2+} influx in HCEC

Fluorescence Ca^{2+} imaging demonstrated intracellular Ca^{2+} increase in HCEC induced by exposure of the cells to 50 ng/ml EGF. There was some variation in the Ca^{2+} response between individual traces, with certain cells displaying large influxes of Ca^{2+} and others showing comparatively smaller Ca^{2+} increases. As a whole, however, a clear upward trend could be observed in the intracellular Ca^{2+} concentration following the introduction of EGF, suggesting a strong interaction between EGFR activation and Ca^{2+} channels in HCEC.

To determine if TRPs are the channels responsible for this EGF-induced effect in HCEC, TRP channel antagonists were tested. These antagonists are often selective to a particular TRP channel or group of TRPs and are used in electrophysiological studies of cells to determine the involvement of certain TRP channel subtypes in an ionic flux (63, 64). If the presence of an antagonist reduces the intracellular Ca^{2+} influx triggered by EGF, it suggests that the TRP channel subtype inhibited by that antagonist is involved in the EGF effect. If the level of EGF-induced Ca^{2+} influx remains unchanged despite the presence of the antagonist, the EGF effect is likely to be independent of the corresponding TRP channel.

One TRP channel antagonist used in this study was BCTC. BCTC is a potent inhibitor of TRPM8 and TRPV1. BCTC has been used to inhibit TRPM8 in various ocular cell types such as in human corneal epithelial as well as endothelial cells (37, 41). In prostate cancer cells, BCTC has exhibited an anti-proliferative effect by inhibiting TRPM8 (65). It has also been shown to reduce thermal hyperalgesia in rats by inhibiting TRPV1 responsible for the detection of pain (66). In this study, fluorescence Ca^{2+} imaging of HCEC in the presence of 10 µM BCTC showed no inhibitory effect on the EGF-induced Ca^{2+} increase, indicating that TRPM8 and TRPV1 are not likely responsible for this phenomenon.

Another TRP channel antagonist used was SKF 96365. SKF 96365 is a non-selective TRP channel antagonist known to inhibit members of the TRPC subfamily. This

imidazole derivative was first characterised as an inhibitor of receptor-mediated Ca^{2+} entry after being found to suppress Ca^{2+} influx stimulated by adenosine diphosphate (ADP) and thrombin in human thrombocytes, neutrophils and endothelial cells. It was also observed to inhibit VDCCs in excitable cells such as GH3 pituitary adenoma cells and arterial smooth muscle cells (67). Subsequently, SKF 96365 was also found to inhibit CCE in HL-60 promyelocytic leukaemia cells (68), thymic lymphocytes (69) and FRTL-5 thyroid epithelial cells (70). Further research into the inhibitor and an increased understanding of TRPs over the years led to a more specific characterisation of SKF 96365 and its effects on TRPC channels in particular. SKF 96365 is now known to inhibit several members of the TRPC subfamily, such as TRPC3 (71, 72), TRPC4 (73), TRPC5 (74), TRPC6 (75, 76) and TRPC7 (77). Fluorescence Ca^{2+} imaging data from this study showed that the EGF-induced Ca^{2+} increase in HCEC was partially reduced in the presence of 10 µM SKF 96365 and completely suppressed in the presence of 20 µM SKF 96365. Based on the known characteristics of SKF 96365, the type of channels responsible for the EGF effect seen in this study can be deduced. As VDCCs are usually activated in response to membrane depolarisation in excitable cells (78), and HCEC are non-excitable cells with no reported activity of VDCCs under physiological conditions, the inhibitory effect of SKF 96365 on VDCCs can be discounted in this present study. The inhibitory effect of SKF 96365 on CCE can also be ignored, as EGF does not appear to trigger CCE in HCEC (see Chapter 4.2). This leaves cell membrane-localised TRPC channels as the likely cause for the EGF-induced Ca^{2+} increase observed in HCEC, an effect which was inhibited in a dose-dependent manner with SKF 96365.

The fluorescence Ca^{2+} imaging results were supported by patch-clamp measurement of whole-cell currents in HCEC. Both inward and outward currents increased in the presence of 50 ng/ml EGF and decreased in the presence of a mixture of 50 ng/ml EGF and 20 µM SKF 96365. This shows that an extracellular application of EGF to HCEC activates ion channels on the cell surface, resulting in an increased flux of ions across the cell membrane. Significant reduction of the EGF-induced inward and outward currents by SKF 96365 confirms that TRPC is the type of channel involved in the process.

TRPC channel activation in response to EGF in HCEC has, in fact, been investigated before. In one previous report, a suppression of EGF-induced currents was observed in HCEC with TRPC4 knocked down (33). This present study provides further evidence for the involvement of TRPC channels in signaling pathways activated by EGF in HCEC.

4.2 EGF effect in HCEC is independent of CCE

In the fluorescence Ca^{2+} imaging experiments, 50 ng/ml EGF did not elicit an intracellular Ca^{2+} increase in HCEC when Ca^{2+} was absent from the extracellular solution. This suggests that intracellular Ca^{2+}-release channel activity and CCE are not involved in the response HCEC to EGF. The intracellular Ca^{2+} increase that occurs in the presence of extracellular Ca^{2+} is likely due to an EGFR-associated activation of TRPC channels on the cell membrane. Although TRPC4 has been reported to be involved in CCE in HCEC and appears to be a key channel involved in the EGF-induced currents in HCEC (33), it is likely that this channel is activated independently of CCE in the presence of EGF. A possible explanation for this is that TRPC4 may have distinct activation mechanisms in HCEC, one involving intracellular Ca^{2+} store depletion and another involving activation of the EGFR. In fact, in existing literature, it has been suggested that TRPC4 is capable of being activated by both store-operated and receptor-operated mechanisms (55).

In cells where CCE is induced by EGF, intracellular Ca^{2+} store depletion is visible as an increase in the fluorescence ratio upon addition of EGF even in the absence of extracellular Ca^{2+}, as observed in RCEC (54). As EGF caused a change in Ca^{2+} fluorescence ratios in HCEC only in the presence of extracellular Ca^{2+}, it can be concluded that activated EGFR in turn activates TRPC channels found on the cell surface of HCEC without mobilisation of Ca^{2+} stores. This is the first time that EGF-induced intracellular Ca^{2+} increase in HCEC is shown to occur independently of CCE.

This finding therefore also reveals a previously unknown difference between the effect of EGF on Ca^{2+} regulation in HCEC and that which has been described in RCEC. It would be advisable to consider this difference when applying rabbit models to study the

effects of EGF-containing drugs on the human corneal epithelium, since distinct intracellular pathways appear to be activated by EGF in the different species.

4.3 Current understanding of TRPC channel association with CCE

This study's demonstration of CCE-independent TRPC channel activation in HCEC is particularly useful as it sheds some light on the complex activity of this lesser understood TRP channel subfamily. While research into the various functions of these channels progresses, evidence continues to accumulate for the involvement of TRPC channels in both CCE-dependent and CCE-independent mechanisms.

In 1995, the first mammalian TRP channel, TRPC1, was identified based on its molecular similarity to the Drosophila TRP channel (79, 80). A year later, other members of the TRPC subfamily, TRPC2-6, were identified (81). TRPC7, the final member of this subfamily, was discovered in 1999 (77). However, unlike the Drosophila TRP channels which are only expressed in insect photoreceptors, mammalian TRPC channels are ubiquitously expressed across a variety of tissues, exhibiting highly diverse properties and functions (82).

Research into TRPC channel activity over the years has often appeared to yield conflicting results, particularly with regard to the channel's involvement in CCE. CCE is the mechanism in which Ca^{2+} channels on the cell membrane are activated by active or passive depletion of intracellular Ca^{2+} stores, resulting in an influx of Ca^{2+} from the extracellular space into the cell (83). In fibroblast-like cells, expression of TRPC1 and TRPC3 were both found to augment CCE, while TRPC2 was found to be activated by store depletion in mice, leading some researchers to propose that TRPC channels were structural components of CCE (81, 84). Similarly, studies have shown that CCE is affected by TRPC1 in chicken DT40 B cells (85) and pulmonary artery smooth muscle cells (PASMC) (86). In HCEC, knockdown of TRPC4 was found to cause a reduction in CCE (33). These observations suggest a relationship between CCE and activity of channels in the TRPC subfamily.

On the other hand, studies have also provided evidence of TRPC channel activity and CCE occurring independently. In one study, TRPC7 appeared not to be involved in

thapsigargin-induced CCE but could be activated by the second messenger diacylglycerol (77). Another report showed that alteration of TRPC channel expression with exogenous hormones such as β-estradiol and trans-retinoic acid produced no effect on CCE in bovine aortic endothelial cells (BAEC) (87). In bovine corneal endothelial cells (BCEC), expression of TRPC4 displayed an inhibitory effect on receptor-induced Ca^{2+} entry but no effect on store-induced Ca^{2+} entry (88). Evidently, the variation in TRPC channel activity under different conditions made it difficult to ascertain the exact function of these channels and their relationship with CCE.

Subsequent research led to the discovery of two cellular components crucial to CCE – stromal interaction molecule 1 (STIM1) and Ca^{2+} release-activated Ca^{2+} channel protein 1 (ORAI1). STIM1 functions as a Ca^{2+} sensor on the ER membrane, while ORAI1 is a pore-forming transmembrane protein whose activation elicits SOC activation on the cell membrane. When the concentration of Ca^{2+} in the ER drops, Ca^{2+} dissociates from the Ca^{2+}-binding domain of STIM1 within the ER lumen. STIM1 then translocates from the ER to punctae near the cell membrane and activates ORAI1, leading to an influx of extracellular Ca^{2+} via SOCs into the cell (89-94). Interestingly, STIM1 and ORAI1 have also been shown to interact with TRPC channels. For instance, STIM1 could activate TRPC1 and TRPC3 (95, 96), while ORAI1 was able to interact with TRPC3 and TRPC6. STIM1 and ORAI1 appear to play regulatory roles closely associated with CCE, in some cases by enabling TRPC channels to activate in response to store depletion (97).

In this present study, CCE-independent activity of TRPC channels was demonstrated. Based on data gathered from fluorescence Ca^{2+} imaging and patch-clamp whole-cell current measurements of HCEC, EGF triggered an influx of Ca^{2+} via TRPC channels on the cell membrane without requiring prior depletion of the intracellular Ca^{2+} stores. Previously, EGF-induced TRPC activation in HCEC was believed to be associated with CCE (33). This study, however, challenges that perspective and highlights the diversity of TRPC channel function. It is likely that while TRPC channel activity may be involved in CCE, the channels can also take part in other intracellular processes which do not necessarily involve CCE in this cell type. Further research, however, is needed to fully

understand the diverse physiological roles that TRPC channels play and their functional differences across the cell types.

4.4 Limitations

In any cell culture, environmental factors may affect the vitality of the cells and compromise their function. In some instances, cells from the HCEC culture were found to undergo apoptosis prematurely, rendering them unsuitable for the experiments. To avoid skewing the results due to such anomalies, the cells were inspected under a light microscope after incubation to ensure that they had maintained their regular form and had successfully proliferated, before conducting the experiments. It should also be noted that measurements were conducted on immortalised cultured cells, which may exhibit different characteristics to cells of primary cultures. To ensure reliability of the experiments, a well-established cell line was used in this study. Cells of this line closely resemble primary HCEC (59). Nevertheless, one should be cautious when using the data obtained from these experiments conducted *in vitro* to predict the characteristics of HCEC *in vivo* due to the differences in external environments.

In fluorescence Ca^{2+} imaging experiments, errors may also arise due to the light-sensitive nature of the process. The wavelength of cell fluorescence measured falls within the range of visible light and is susceptible to interference from external light sources. Furthermore, photobleaching may occur in the fluorescence dye Fura-2AM when exposed to light at a high intensities or for a prolonged period of time (98). This can alter its spectral properties and give rise to inaccuracies when measuring the levels of intracellular Ca^{2+}. To counter these effects, the dye-stained cells were stored in the dark, while measurements with the fluorescence microscope were carried out with as little ambient light as possible. Nevertheless, a small amount of external light exposure is to be expected due to operational constraints.

The patch-clamp technique is also associated with certain limitations. As each measurement is performed on a single cell, the accuracy of the measured whole-cell currents is highly dependent on the quality of cell culture and cell preparation. In addition, the possibility of a weak seal between the cell and the microchip during

measurements is a technical limitation of the process. If the seal is not stable enough, leak currents may become significant and interfere with the recording of whole-cell currents. To ensure more accurate results, the experiments were only allowed to proceed if the seal resistance was sufficiently high. Leak currents were also compensated for and cells with high leak currents were excluded from the analysis.

4.5 Clinical application

Knowing the effect of EGF on the corneal epithelium is of great medical importance. EGF is physiologically present in healthy tears and plays a vital role in maintaining the integrity of the ocular surface (99, 100). However, in patients with dry eye syndrome (DES), tear production and consequently, the amount of EGF present naturally on the cornea, is reduced. This loss of this protective EGF could cause the cornea to become prone to defects as its wound-healing capacity is affected. Interestingly, one study demonstrated that topically applied EGF was able to improve the symptoms of patients with persistent corneal epithelial defects (101). In addition, many types of artificial tears which are used to treat conditions such as DES contain hydrogels which activate the EGFR. This mechanism is thought to be partly responsible for the healing properties of such products (102).

Even cancer patients undergoing treatments with EGFR antibodies appear to benefit from a topical application EGF to the cornea (103). Monoclonal antibodies such as cetuximab, which inhibit the EGFR, are often used in the treatment of cancers like colorectal, head and neck carcinomas. However, while effective in the reduction of the tumours, these antibodies may also inhibit the useful healing effect of EGF in the cornea. In such patients, application of EGF directly to the ocular surface has been shown to reduce the side effects of EGFR antibodies on the corneal epithelium (103).

EGF, with its wide-ranging applications, shows great promise as a therapeutic option in a host of ocular diseases. In order to understand and take full advantage of the healing properties of this growth factor, it is important to know the intracellular changes brought about by EGFR activation. It is hoped that this study facilitates a clearer understanding

of the complex interactions of EGFR with TRPs in corneal cells and paves the way for the development of specific drugs to better treat pathologies of the cornea in the future.

References

1. DelMonte DW, Kim T. Anatomy and physiology of the cornea. J Cataract Refract Surg. 2011;37(3):588-98.

2. Sridhar MS. Anatomy of cornea and ocular surface. Indian J Ophthalmol. 2018;66(2):190-4.

3. Masterton S, Ahearne M. Mechanobiology of the corneal epithelium. Exp Eye Res. 2018;177:122-9.

4. Klyce SD. Enhancing fluid secretion by the corneal epithelium. Invest Ophthalmol Vis Sci. 1977;16(10):968-73.

5. Candia OA, Zamudio AC. Chloride-activated water permeability in the frog corneal epithelium. J Membr Biol. 1995;143(3):259-66.

6. Maurice DM. The location of the fluid pump in the cornea. J Physiol. 1972;221(1):43-54.

7. Hong SC, Ha JH, Lee JK, Jung SH, Kim JC. In Vivo Anti-Inflammation Potential of Aster koraiensis Extract for Dry Eye Syndrome by the Protection of Ocular Surface. Nutrients. 2020;12(11).

8. Stern ME, Schaumburg CS, Pflugfelder SC. Dry eye as a mucosal autoimmune disease. Int Rev Immunol. 2013;32(1):19-41.

9. Wei Y, Asbell PA. The core mechanism of dry eye disease is inflammation. Eye Contact Lens. 2014;40(4):248-56.

10. Li H, Zhang J, Kumar A, Zheng M, Atherton SS, Yu FS. Herpes simplex virus 1 infection induces the expression of proinflammatory cytokines, interferons and TLR7 in human corneal epithelial cells. Immunology. 2006;117(2):167-76.

11. Li S, Zhou J, Zhang L, Li J, Yu J, Ning K, Qu Y, He H, Chen Y, Reinach PS, Liu CY, Liu Z, Li W. Ectodysplasin A regulates epithelial barrier function through sonic hedgehog signalling pathway. J Cell Mol Med. 2018;22(1):230-40.

12. Sangwan VS. Limbal stem cells in health and disease. Biosci Rep. 2001;21(4):385-405.

13. Ahmad S, Osei-Bempong C, Dana R, Jurkunas U. The culture and transplantation of human limbal stem cells. J Cell Physiol. 2010;225(1):15-9.

14. Ahmad S, Figueiredo F, Lako M. Corneal epithelial stem cells: characterization, culture and transplantation. Regen Med. 2006;1(1):29-44.

15. Vaidyanathan U, Hopping GC, Liu HY, Somani AN, Ronquillo YC, Hoopes PC, Moshirfar M. Persistent Corneal Epithelial Defects: A Review Article. Med Hypothesis Discov Innov Ophthalmol. 2019;8(3):163-76.

16. Utine CA, Stern M, Akpek EK. Clinical review: topical ophthalmic use of cyclosporin A. Ocul Immunol Inflamm. 2010;18(5):352-61.

17. Holland EJ, Olsen TW, Ketcham JM, Florine C, Krachmer JH, Purcell JJ, Lam S, Tessler HH, Sugar J. Topical cyclosporin A in the treatment of anterior segment inflammatory disease. Cornea. 1993;12(5):413-9.

18. Nanji AA, Sayyad FE, Karp CL. Topical chemotherapy for ocular surface squamous neoplasia. Curr Opin Ophthalmol. 2013;24(4):336-42.

19. Gurnani B, Kaur K. Ocular Surface Squamous Neoplasia. StatPearls. Treasure Island (FL)2022.

20. Chen Z, You J, Liu X, Cooper S, Hodge C, Sutton G, Crook JM, Wallace GG. Biomaterials for corneal bioengineering. Biomed Mater. 2018;13(3):032002.

21. Brini M, Cali T, Ottolini D, Carafoli E. Intracellular calcium homeostasis and signaling. Met Ions Life Sci. 2013;12:119-68.

22. Masterton S, Ahearne M. The Effect of Calcium and Glucose Concentration on Corneal Epithelial Cell Lines Differentiation, Proliferation, and Focal Adhesion Expression. Biores Open Access. 2019;8(1):74-83.

23. Mergler S, Garreis F, Sahlmuller M, Reinach PS, Paulsen F, Pleyer U. Thermosensitive transient receptor potential channels in human corneal epithelial cells. J Cell Physiol. 2011;226(7):1828-42.

24. Duncan G, Collison DJ. Calcium signalling in ocular tissues: functional activity of G-protein and tyrosine-kinase coupled receptors. Exp Eye Res. 2002;75(4):377-89.

25. Van Petegem F. Ryanodine receptors: structure and function. J Biol Chem. 2012;287(38):31624-32.

26. Wu X, Yang H, Iserovich P, Fischbarg J, Reinach PS. Regulatory volume decrease by SV40-transformed rabbit corneal epithelial cells requires ryanodine-sensitive Ca2+-induced Ca2+ release. J Membr Biol. 1997;158(2):127-36.

27. Venkatachalam K, Montell C. TRP channels. Annu Rev Biochem. 2007;76:387-417.

28. Reinach PS, Mergler S, Okada Y, Saika S. Ocular transient receptor potential channel function in health and disease. BMC Ophthalmol. 2015;15 Suppl 1:153.

29. Caterina MJ, Schumacher MA, Tominaga M, Rosen TA, Levine JD, Julius D. The capsaicin receptor: a heat-activated ion channel in the pain pathway. Nature. 1997;389(6653):816-24.

30. Tominaga M, Caterina MJ, Malmberg AB, Rosen TA, Gilbert H, Skinner K, Raumann BE, Basbaum AI, Julius D. The cloned capsaicin receptor integrates multiple pain-producing stimuli. Neuron. 1998;21(3):531-43.

31. Pan Z, Wang Z, Yang H, Zhang F, Reinach PS. TRPV1 activation is required for hypertonicity-stimulated inflammatory cytokine release in human corneal epithelial cells. Invest Ophthalmol Vis Sci. 2011;52(1):485-93.

32. Tominaga M. Nociception and TRP channels. Handb Exp Pharmacol. 2007(179):489-505.

33. Yang H, Mergler S, Sun X, Wang Z, Lu L, Bonanno JA, Pleyer U, Reinach PS. TRPC4 knockdown suppresses epidermal growth factor-induced store-operated channel activation and growth in human corneal epithelial cells. J Biol Chem. 2005;280(37):32230-7.

34. Zhang F, Yang H, Wang Z, Mergler S, Liu H, Kawakita T, Tachado SD, Pan Z, Capo-Aponte JE, Pleyer U, Koziel H, Kao WW, Reinach PS. Transient receptor potential vanilloid 1 activation induces inflammatory cytokine release in corneal epithelium through MAPK signaling. J Cell Physiol. 2007;213(3):730-9.

35. Yamada T, Ueda T, Ugawa S, Ishida Y, Imayasu M, Koyama S, Shimada S. Functional expression of transient receptor potential vanilloid 3 (TRPV3) in corneal epithelial cells: involvement in thermosensation and wound healing. Exp Eye Res. 2010;90(1):121-9.

36. Pan Z, Yang H, Mergler S, Liu H, Tachado SD, Zhang F, Kao WW, Koziel H, Pleyer U, Reinach PS. Dependence of regulatory volume decrease on transient receptor potential vanilloid 4 (TRPV4) expression in human corneal epithelial cells. Cell Calcium. 2008;44(4):374-85.

37. Lucius A, Khajavi N, Reinach PS, Kohrle J, Dhandapani P, Huimann P, Ljubojevic N, Grotzinger C, Mergler S. 3-Iodothyronamine increases transient receptor potential melastatin channel 8 (TRPM8) activity in immortalized human corneal epithelial cells. Cell Signal. 2016;28(3):136-47.

38. Khajavi N, Reinach PS, Slavi N, Skrzypski M, Lucius A, Strauss O, Kohrle J, Mergler S. Thyronamine induces TRPM8 channel activation in human conjunctival epithelial cells. Cell Signal. 2015;27(2):315-25.

39. Mergler S, Garreis F, Sahlmuller M, Lyras EM, Reinach PS, Dwarakanath A, Paulsen F, Pleyer U. Calcium regulation by thermo- and osmosensing transient receptor potential vanilloid channels (TRPVs) in human conjunctival epithelial cells. Histochem Cell Biol. 2012;137(6):743-61.

40. Mergler S, Valtink M, Coulson-Thomas VJ, Lindemann D, Reinach PS, Engelmann K, Pleyer U. TRPV channels mediate temperature-sensing in human corneal endothelial cells. Exp Eye Res. 2010;90(6):758-70.

41. Mergler S, Mertens C, Valtink M, Reinach PS, Szekely VC, Slavi N, Garreis F, Abdelmessih S, Turker E, Fels G, Pleyer U. Functional significance of thermosensitive transient receptor potential melastatin channel 8 (TRPM8) expression in immortalized human corneal endothelial cells. Exp Eye Res. 2013;116:337-49.

42. Turker E, Garreis F, Khajavi N, Reinach PS, Joshi P, Brockmann T, Lucius A, Ljubojevic N, Turan E, Cooper D, Schick F, Reinholz R, Pleyer U, Kohrle J, Mergler S. Vascular Endothelial Growth Factor (VEGF) Induced Downstream Responses to Transient Receptor Potential Vanilloid 1 (TRPV1) and 3-Iodothyronamine (3-T1AM) in Human Corneal Keratocytes. Front Endocrinol (Lausanne). 2018;9:670.

43. Ferreira G, Raddatz N, Lorenzo Y, González C, Latorre R. Biophysical and Molecular Features of Thermosensitive TRP Channels Involved in Sensory Transduction. In: Madrid R, Bacigalupo J, editors. TRP Channels in Sensory Transduction. Cham (CH): Springer International Publishing; 2015. p. 1-39.

44. Savage CR, Jr., Inagami T, Cohen S. The primary structure of epidermal growth factor. J Biol Chem. 1972;247(23):7612-21.

45. Dawson JP, Berger MB, Lin CC, Schlessinger J, Lemmon MA, Ferguson KM. Epidermal growth factor receptor dimerization and activation require ligand-induced conformational changes in the dimer interface. Mol Cell Biol. 2005;25(17):7734-42.

46. Herbst RS. Review of epidermal growth factor receptor biology. Int J Radiat Oncol Biol Phys. 2004;59(2 Suppl):21-6.

47. Pastor JC, Calonge M. Epidermal growth factor and corneal wound healing. A multicenter study. Cornea. 1992;11(4):311-4.

48. Yanai R, Yamada N, Inui M, Nishida T. Correlation of proliferative and anti-apoptotic effects of HGF, insulin, IGF-1, IGF-2, and EGF in SV40-transformed human corneal epithelial cells. Exp Eye Res. 2006;83(1):76-83.

49. Peterson JL, Ceresa BP. Epidermal Growth Factor Receptor Expression in the Corneal Epithelium. Cells. 2021;10(9).

50. P OC, Rhys-Evans P, Modjtahedi H, Court W, Box G, Eccles S. Overexpression of epidermal growth factor receptor in human head and neck squamous carcinoma cell lines correlates with matrix metalloproteinase-9 expression and in vitro invasion. Int J Cancer. 2000;86(3):307-17.

51. Fabricant RN, Alpar AJ, Centifanto YM, Kaufman HE. Epidermal growth factor receptors on corneal endothelium. Arch Ophthalmol. 1981;99(2):305-8.

52. Yang SG, Hollenberg MD. Distinct receptors for epidermal growth factor-urogastrone in cultured gastric smooth muscle cells. Am J Physiol. 1991;260(6 Pt 1):G827-34.

53. Zieske JD, Takahashi H, Hutcheon AE, Dalbone AC. Activation of epidermal growth factor receptor during corneal epithelial migration. Invest Ophthalmol Vis Sci. 2000;41(6):1346-55.

54. Yang H, Sun X, Wang Z, Ning G, Zhang F, Kong J, Lu L, Reinach PS. EGF stimulates growth by enhancing capacitative calcium entry in corneal epithelial cells. J Membr Biol. 2003;194(1):47-58.

55. Odell AF, Scott JL, Van Helden DF. Epidermal growth factor induces tyrosine phosphorylation, membrane insertion, and activation of transient receptor potential channel 4. J Biol Chem. 2005;280(45):37974-87.

56. Hisatsune C, Kuroda Y, Nakamura K, Inoue T, Nakamura T, Michikawa T, Mizutani A, Mikoshiba K. Regulation of TRPC6 channel activity by tyrosine phosphorylation. J Biol Chem. 2004;279(18):18887-94.

57. Tajeddine N, Gailly P. TRPC1 protein channel is major regulator of epidermal growth factor receptor signaling. J Biol Chem. 2012;287(20):16146-57.

58. Schaefer M, Plant TD, Obukhov AG, Hofmann T, Gudermann T, Schultz G. Receptor-mediated regulation of the nonselective cation channels TRPC4 and TRPC5. J Biol Chem. 2000;275(23):17517-26.

59. Araki-Sasaki K, Ohashi Y, Sasabe T, Hayashi K, Watanabe H, Tano Y, Handa H. An SV40-immortalized human corneal epithelial cell line and its characterization. Invest Ophthalmol Vis Sci. 1995;36(3):614-21.

60. Grynkiewicz G, Poenie M, Tsien RY. A new generation of Ca2+ indicators with greatly improved fluorescence properties. J Biol Chem. 1985;260(6):3440-50.

61. Caruso C, Costagliola C, Troisi S, Epstein RL. Compaction of very thin corneas from ultraviolet A riboflavin-vitamin E transepithelial cross-linking. Exp Eye Res. 2021;205:108484.

62. Barry PH. JPCalc, a software package for calculating liquid junction potential corrections in patch-clamp, intracellular, epithelial and bilayer measurements and for correcting junction potential measurements. J Neurosci Methods. 1994;51(1):107-16.

63. Vriens J, Appendino G, Nilius B. Pharmacology of vanilloid transient receptor potential cation channels. Mol Pharmacol. 2009;75(6):1262-79.

64. Bon RS, Wright DJ, Beech DJ, Sukumar P. Pharmacology of TRPC Channels and Its Potential in Cardiovascular and Metabolic Medicine. Annu Rev Pharmacol Toxicol. 2022;62:427-46.

65. Liu T, Fang Z, Wang G, Shi M, Wang X, Jiang K, Yang Z, Cao R, Tao H, Wang X, Zhou J. Anti-tumor activity of the TRPM8 inhibitor BCTC in prostate cancer DU145 cells. Oncol Lett. 2016;11(1):182-8.

66. Tekus V, Bolcskei K, Kis-Varga A, Dezsi L, Szentirmay E, Visegrady A, Horvath C, Szolcsanyi J, Petho G. Effect of transient receptor potential vanilloid 1 (TRPV1) receptor antagonist compounds SB705498, BCTC and AMG9810 in rat models of

thermal hyperalgesia measured with an increasing-temperature water bath. Eur J Pharmacol. 2010;641(2-3):135-41.

67. Merritt JE, Armstrong WP, Benham CD, Hallam TJ, Jacob R, Jaxa-Chamiec A, Leigh BK, McCarthy SA, Moores KE, Rink TJ. SK&F 96365, a novel inhibitor of receptor-mediated calcium entry. Biochem J. 1990;271(2):515-22.

68. Demaurex N, Lew DP, Krause KH. Cyclopiazonic acid depletes intracellular Ca2+ stores and activates an influx pathway for divalent cations in HL-60 cells. J Biol Chem. 1992;267(4):2318-24.

69. Mason MJ, Mayer B, Hymel LJ. Inhibition of Ca2+ transport pathways in thymic lymphocytes by econazole, miconazole, and SKF 96365. Am J Physiol. 1993;264(3 Pt 1):C654-62.

70. Tornquist K. Activation of calcium entry by cyclopiazonic acid in thyroid FRTL-5 cells. Cell Calcium. 1993;14(5):411-7.

71. Zhu X, Jiang M, Birnbaumer L. Receptor-activated Ca2+ influx via human Trp3 stably expressed in human embryonic kidney (HEK)293 cells. Evidence for a non-capacitative Ca2+ entry. J Biol Chem. 1998;273(1):133-42.

72. Liu D, Scholze A, Zhu Z, Kreutz R, Wehland-von-Trebra M, Zidek W, Tepel M. Increased transient receptor potential channel TRPC3 expression in spontaneously hypertensive rats. Am J Hypertens. 2005;18(11):1503-7.

73. Kinoshita M, Akaike A, Satoh M, Kaneko S. Positive regulation of capacitative Ca2+ entry by intracellular Ca2+ in Xenopus oocytes expressing rat TRP4. Cell Calcium. 2000;28(3):151-9.

74. Okada T, Shimizu S, Wakamori M, Maeda A, Kurosaki T, Takada N, Imoto K, Mori Y. Molecular cloning and functional characterization of a novel receptor-activated TRP Ca2+ channel from mouse brain. J Biol Chem. 1998;273(17):10279-87.

75. Boulay G, Zhu X, Peyton M, Jiang M, Hurst R, Stefani E, Birnbaumer L. Cloning and expression of a novel mammalian homolog of Drosophila transient receptor

potential (Trp) involved in calcium entry secondary to activation of receptors coupled by the Gq class of G protein. J Biol Chem. 1997;272(47):29672-80.

76. Anderson M, Roshanravan H, Khine J, Dryer SE. Angiotensin II activation of TRPC6 channels in rat podocytes requires generation of reactive oxygen species. J Cell Physiol. 2014;229(4):434-42.

77. Okada T, Inoue R, Yamazaki K, Maeda A, Kurosaki T, Yamakuni T, Tanaka I, Shimizu S, Ikenaka K, Imoto K, Mori Y. Molecular and functional characterization of a novel mouse transient receptor potential protein homologue TRP7. Ca(2+)-permeable cation channel that is constitutively activated and enhanced by stimulation of G protein-coupled receptor. J Biol Chem. 1999;274(39):27359-70.

78. Harraz OF, Altier C. STIM1-mediated bidirectional regulation of Ca(2+) entry through voltage-gated calcium channels (VGCC) and calcium-release activated channels (CRAC). Front Cell Neurosci. 2014;8:43.

79. Wes PD, Chevesich J, Jeromin A, Rosenberg C, Stetten G, Montell C. TRPC1, a human homolog of a Drosophila store-operated channel. Proc Natl Acad Sci U S A. 1995;92(21):9652-6.

80. Zhu X, Chu PB, Peyton M, Birnbaumer L. Molecular cloning of a widely expressed human homologue for the Drosophila trp gene. FEBS Lett. 1995;373(3):193-8.

81. Zhu X, Jiang M, Peyton M, Boulay G, Hurst R, Stefani E, Birnbaumer L. trp, a novel mammalian gene family essential for agonist-activated capacitative Ca2+ entry. Cell. 1996;85(5):661-71.

82. Wang H, Cheng X, Tian J, Xiao Y, Tian T, Xu F, Hong X, Zhu MX. TRPC channels: Structure, function, regulation and recent advances in small molecular probes. Pharmacol Ther. 2020;209:107497.

83. Putney JW, Jr. A model for receptor-regulated calcium entry. Cell Calcium. 1986;7(1):1-12.

84. Vannier B, Peyton M, Boulay G, Brown D, Qin N, Jiang M, Zhu X, Birnbaumer L. Mouse trp2, the homologue of the human trpc2 pseudogene, encodes mTrp2, a store depletion-activated capacitative Ca2+ entry channel. Proc Natl Acad Sci U S A. 1999;96(5):2060-4.

85. Mori Y, Wakamori M, Miyakawa T, Hermosura M, Hara Y, Nishida M, Hirose K, Mizushima A, Kurosaki M, Mori E, Gotoh K, Okada T, Fleig A, Penner R, Iino M, Kurosaki T. Transient receptor potential 1 regulates capacitative Ca(2+) entry and Ca(2+) release from endoplasmic reticulum in B lymphocytes. J Exp Med. 2002;195(6):673-81.

86. Sweeney M, Yu Y, Platoshyn O, Zhang S, McDaniel SS, Yuan JX. Inhibition of endogenous TRP1 decreases capacitative Ca2+ entry and attenuates pulmonary artery smooth muscle cell proliferation. Am J Physiol Lung Cell Mol Physiol. 2002;283(1):L144-55.

87. Chang AS, Chang SM, Garcia RL, Schilling WP. Concomitant and hormonally regulated expression of trp genes in bovine aortic endothelial cells. FEBS Lett. 1997;415(3):335-40.

88. Xie Q, Zhang Y, Cai Sun X, Zhai C, Bonanno JA. Expression and functional evaluation of transient receptor potential channel 4 in bovine corneal endothelial cells. Exp Eye Res. 2005;81(1):5-14.

89. Roos J, DiGregorio PJ, Yeromin AV, Ohlsen K, Lioudyno M, Zhang S, Safrina O, Kozak JA, Wagner SL, Cahalan MD, Velicelebi G, Stauderman KA. STIM1, an essential and conserved component of store-operated Ca2+ channel function. J Cell Biol. 2005;169(3):435-45.

90. Zhang SL, Yu Y, Roos J, Kozak JA, Deerinck TJ, Ellisman MH, Stauderman KA, Cahalan MD. STIM1 is a Ca2+ sensor that activates CRAC channels and migrates from the Ca2+ store to the plasma membrane. Nature. 2005;437(7060):902-5.

91. Liou J, Kim ML, Heo WD, Jones JT, Myers JW, Ferrell JE, Jr., Meyer T. STIM is a Ca2+ sensor essential for Ca2+-store-depletion-triggered Ca2+ influx. Curr Biol. 2005;15(13):1235-41.

92. Feske S, Gwack Y, Prakriya M, Srikanth S, Puppel SH, Tanasa B, Hogan PG, Lewis RS, Daly M, Rao A. A mutation in Orai1 causes immune deficiency by abrogating CRAC channel function. Nature. 2006;441(7090):179-85.

93. Vig M, Peinelt C, Beck A, Koomoa DL, Rabah D, Koblan-Huberson M, Kraft S, Turner H, Fleig A, Penner R, Kinet JP. CRACM1 is a plasma membrane protein essential for store-operated Ca2+ entry. Science. 2006;312(5777):1220-3.

94. Zhang SL, Yeromin AV, Zhang XH, Yu Y, Safrina O, Penna A, Roos J, Stauderman KA, Cahalan MD. Genome-wide RNAi screen of Ca(2+) influx identifies genes that regulate Ca(2+) release-activated Ca(2+) channel activity. Proc Natl Acad Sci U S A. 2006;103(24):9357-62.

95. Huang GN, Zeng W, Kim JY, Yuan JP, Han L, Muallem S, Worley PF. STIM1 carboxyl-terminus activates native SOC, I(crac) and TRPC1 channels. Nat Cell Biol. 2006;8(9):1003-10.

96. Zeng W, Yuan JP, Kim MS, Choi YJ, Huang GN, Worley PF, Muallem S. STIM1 gates TRPC channels, but not Orai1, by electrostatic interaction. Mol Cell. 2008;32(3):439-48.

97. Liao Y, Erxleben C, Yildirim E, Abramowitz J, Armstrong DL, Birnbaumer L. Orai proteins interact with TRPC channels and confer responsiveness to store depletion. Proc Natl Acad Sci U S A. 2007;104(11):4682-7.

98. Becker PL, Fay FS. Photobleaching of fura-2 and its effect on determination of calcium concentrations. Am J Physiol. 1987;253(4 Pt 1):C613-8.

99. Ohashi Y, Motokura M, Kinoshita Y, Mano T, Watanabe H, Kinoshita S, Manabe R, Oshiden K, Yanaihara C. Presence of epidermal growth factor in human tears. Invest Ophthalmol Vis Sci. 1989;30(8):1879-82.

100. van Setten GB, Viinikka L, Tervo T, Pesonen K, Tarkkanen A, Perheentupa J. Epidermal growth factor is a constant component of normal human tear fluid. Graefes Arch Clin Exp Ophthalmol. 1989;227(2):184-7.

101. Moon HS, Li L, Yoon HJ, Ji YS, Yoon KC. Effect of epidermal growth factor ointment on persistent epithelial defects of the cornea. BMC Ophthalmol. 2020;20(1):147.

102. Lozano JS, Chay EY, Healey J, Sullenberger R, Klarlund JK. Activation of the epidermal growth factor receptor by hydrogels in artificial tears. Exp Eye Res. 2008;86(3):500-5.

103. Forster CG, Cursiefen C, Kruse FE. [Topical application of EGF for the therapy of persisting corneal erosion under cetuximab treatment]. Ophthalmologe. 2008;105(3):269-73.

Statutory Declaration

“I, Julian Francisco Lopez, by personally signing this document in lieu of an oath, hereby affirm that I prepared the submitted dissertation on the topic Epidermal growth factor (EGF) induces activation of transient receptor potential canonical (TRPC) channels in cultured human corneal epithelial cells (HCEC) / Epidermaler Wachstumsfaktor (EGF) induziert die Aktivierung von kanonischen Transient-Receptor-Potential (TRPC)-Kanälen in kultivierten humanen Hornhautepithelzellen (HCEC), independently and without the support of third parties, and that I used no other sources and aids than those stated.

All parts which are based on the publications or presentations of other authors, either in letter or in spirit, are specified as such in accordance with the citing guidelines. The sections on methodology (in particular regarding practical work, laboratory regulations, statistical processing) and results (in particular regarding figures, charts and tables) are exclusively my responsibility.

Furthermore, I declare that I have correctly marked all of the data, the analyses, and the conclusions generated from data obtained in collaboration with other persons, and that I have correctly marked my own contribution and the contributions of other persons (cf. declaration of contribution). I have correctly marked all texts or parts of texts that were generated in collaboration with other persons.

My contributions to any publications to this dissertation correspond to those stated in the below joint declaration made together with the supervisor. All publications created within the scope of the dissertation comply with the guidelines of the ICMJE (International Committee of Medical Journal Editors; www.icmje.org) on authorship. In addition, I declare that I shall comply with the regulations of Charité – Universitätsmedizin Berlin on ensuring good scientific practice.

I declare that I have not yet submitted this dissertation in identical or similar form to another Faculty.

The significance of this statutory declaration and the consequences of a false statutory declaration under criminal law (Sections 156, 161 of the German Criminal Code) are known to me.”

Date Signature

Curriculum vitae

My curriculum vitae does not appear in the electronic version of my paper for reasons of data protection.

Acknowledgments

Throughout the course of this study, many people have generously rendered their assistance in one way or another. Although impossible to list them all here, I am immensely grateful for their support.

My sincerest gratitude to my doctoral advisor, PD Dr. phil. nat. Stefan Mergler, for his tireless contribution of ideas, advice and encouragement, and for providing the lab and materials necessary for the research. Dr. Mergler's exemplary dedication to teaching and his genuine concern for the well-being of his students have certainly left a lasting impression on all who have had the privilege of being taught by him.

I am grateful to my second doctoral advisor, Prof. Dr. rer. nat. Heike Biebermann, for taking the time to advice on the direction of this study.

I am also thankful to PD Dr. rer. medic. Monika Valtink for supporting the study by conducting preliminary research on TRPs.

I appreciate the advice of Dr. Peter S. Reinach, expert in ocular TRP channel research.

My heartfelt thanks to the many students, interns and other members of the lab for their assistance with the experiments.

Finally, my warmest gratitude to Sarah and Wilfrid Lopez for their unwavering support every step of the way, without which this venture would not have been possible.